The Cryosphere
Discussions
Open Access
EGU

Dynamical response of the southwestern Laurentide Ice Sheet to rapid Bølling-Allerød warming

Sophie L. Norris[1,2*], Martin Margold[3], David J. A. Evans[4], Nigel Atkinson[5] and Duane G. Froese[2*]

5 [1]Department of Geography, University of Victoria, David Turpin Building, 3800 Finnerty Road, Victoria, BC, V9P 5C2, Canada
[2]Department of Earth and Atmospheric Sciences, 1-26 Earth Sciences Building, University of Alberta, Edmonton, AB, T6G 2E3, Canada
[3]Department of Physical Geography and Geoecology, Charles University, Albertov 6, 128 43 Praha 2, Czech Republic
[4]Department of Geography, Durham University, South Road, Durham, DH1 3LE, United Kingdom
10 [5]Alberta Geological Survey, Alberta Energy Regulator, 402 Twin Atria Building, 4 4999-98 Avenue, Edmonton, AB, T6B 2X3, Canada
*Corresponding authors

Correspondence to: Sophie L. Norris (sophienorris@uvic.ca) and Duane G. Froese (duane.froese@ualberta.ca)

Abstract

15 The climatic transition from the Last Glacial Maximum (LGM) to the early Holocene (ca. 18-12 ka BP) involved rates of temperature change comparable with present-day warming trends. The most rapid recorded changes in temperature occurred during the abrupt climate oscillations known as the Bølling-Allerød interstadial (14.7-12.9 ka BP) and the Younger Dryas stadial (12.9-11.7 ka BP). Accurate reconstructions of ice sheet behaviour during these climate oscillations provide the opportunity to assess long-term ice sheet evolution in reaction to a rapidly changing climate. Here, we use glacial geomorphological inverse methods 20 (flowsets) to reconstruct the ice flow dynamics associated with changes in ice stream catchments (ice divides and domes) and the marginal retreat pattern of the southwestern sector of the Laurentide Ice Sheet (SWLIS). We combine this ice dynamic reconstruction with a recently compiled regional deglaciation chronology to present a model of ice sheet behaviour spanning pre-LGM to the early Holocene. Our reconstruction depicts rapid ice geometry changes, including three macroscale reorganizations of the ice drainage network followed by regional deglaciation synchronous with abrupt warming during the Bølling-Allerød 25 interstadial. Initial westward flow is documented, most probably associated with an evolving ice stream network during the advance to the LGM. Ice streaming at the LGM was marked by southward flows, unconstrained by topography. Following this, a significant switch in the ice sheets dynamics occurred at ~15 ka BP to topographically controlled south-eastward flow constrained by preglacial-valley systems. This was replaced by a second switch in ice flow orientation to the southwest at ~14.5 ka BP. Rates of ice sheet retreat then slowed considerably during the Younger Dryas stadial; at this time, the ice margin was situated north of 30 the Canadian Shield boundary and ice flow continued to be sourced from the northeast. Resulting from these changes in ice sheet dynamics, we recognize a pattern of deglacial landform zonation within the SWLIS characterized by active ice margin recession and ice sheet stagnation and downwasting punctuated by local surging (terrestrial ice sheet collapse): (1) the outer deglacial zone is characterized by large recessional moraines aligned with the direction of active ice margin retreat; (2) the intermediate deglacial zone contains large regions of hummocky and stagnation terrain, in some areas overprinted by the signature of local surges, 35 reflecting punctuated stagnation and downwasting and; (3) the inner deglacial zone comprises inset recessional moraines demarcating progressive regional ice margin retreat. We attribute these macroscale changes in ice flow geometry and the associated deglacial behaviour to external climatic forcing during the Bølling-Allerød and Younger Dryas but also recognize the role of internal (glaciological, lithological and topographic) controls.

1 Introduction

Mass loss from contemporary ice sheets to global sea-level rise has accelerated over the last three decades, mainly resulting from enhanced ice-flow rates and changes in surface mass balance, broadly linked to atmospheric and oceanic warming (Alley et al., 2005; Rignot and Kanagaratnam, 2006; Rignot et al., 2008, 2011; Shepherd, 2018). Changes in ice sheet dynamics are of particular concern given the potential sea level equivalent contribution of ice sheets in Greenland and Antarctica (Pattyn et al., 2018). However, with current observations only spanning a few decades, significant uncertainties remain in projecting an ice sheet's response to future climate system changes. Consequently, reconstructing palaeo-ice sheet behaviour in response to past climatic fluctuations is important to assess future changes to contemporary ice sheets (Alley and Bindschadler, 2001; Rignot and Thomas, 2002; Clark et al., 2009; Carlson and Clark, 2012).

In this context, the complex and largely well-preserved landform imprint of the Late Wisconsinan Laurentide Ice Sheet (LIS) documents regional palaeoglaciological responses to rapid climate change during the last deglaciation (ca. 18-12 ka BP) and consequently is recognized as a valuable information source (Dyke and Prest, 1987; Clark, 1994; Dyke, 2004; Margold et al., 2015b; Stokes et al., 2016; Margold et al., 2018). In particular, geomorphic and sedimentary investigations of parts of the southwestern LIS (SWLIS) have documented major ice flow reorganizations (Ross et al., 2009; Ó Cofaigh et al., 2010; Evans et al., 2014; Atkinson et al., 2016; Fig 1). However, until recently, large discrepancies between different chronological methods have led to uncertainties surrounding the timing of these reorganizations and, thus how they relate to external climate forcing. An updated deglacial chronology (Norris et al., 2022), comprising a synthesis of ~150 [10]Be terrestrial cosmogenic nuclide exposure, radiocarbon and infrared/optically stimulated luminescence dates, indicates that the SWLIS underwent rapid deglaciation in response to warming during the Bølling-Allerød (BA) interstadial (14.7-12.9 ka BP; Rasmussen et al., 2014) followed by a decrease in ice sheet retreat rates and marginal stand-still during the Younger Dryas (YD) stadial. Here, we use glacial geomorphological mapping followed by the classification of individual features into flowsets to reconstruct the ice flow dynamics associated with changes in ice stream catchments (ice divides and domes) and the marginal retreat pattern of the SWLIS. We combine this ice dynamic reconstruction with pre-existing chronologies to present a model of ice sheet behaviour spanning pre-Last Glacial Maximum (LGM) to the early Holocene.

Our reconstruction supports previous assertions of a complex and evolving network of ice flow during the last deglaciation. We propose that these dynamical changes are the product of three macroscale ice flow reorganizations within a ~2500 yr interval accompanied by rapid ice margin retreat and ice margin stagnation (in some areas punctuated by local surging). We attribute these macroscale changes in ice flow dynamics, in large part, to climatic changes during the BA and YD. However, we also highlight the complex interplay between this external driving mechanism and internal glaciological, lithological, and topographic controls. Importantly, our reconstruction also demonstrates that macroscale changes in ice sheet dynamics that occur in response to external climate forcing are not limited to marine-based ice marginal settings but also occur at terrestrial ice sheet margins.

2 Study area and previous work

2.1 Physiographic setting and surficial geology

Our study encompasses the SWLIS from the southern Rocky Mountain Foothills to the Canadian Shield. Ice flowing from the Keewatin Ice Dome fed this sector, where it converged with the Cordilleran Ice Sheet (CIS) to the west and extended into the

northwestern United States (Fig. 1). This portion of the ice sheet covered two broad physiographic zones: the Interior Plains to the south and the Canadian Shield to the northeast. The region is underlain by crystalline Precambrian rocks that outcrop in the northern Shield region. These basement rocks are overlain in the south by sedimentary units occupying the Western Canada Sedimentary

80 Basin, which thickens to the southwest, forming a >5000 m thick wedge near the eastern foothills (Mossop and Shetsen, 2012; Banks and Harris, 2018). Bordering the eastern foothills of the Rocky Mountains, the SWLIS subsumed several uplands, which are composed of bedrock remnants of Cretaceous shales and sandstones (Andriashek and Barendregt, 2017). Large preglacial valley systems separate these uplands and are composed of thick (up to ~350 m) Quaternary sequences of diamict, glaciofluvial sand and gravel and glaciolacustrine silts and clays (Stalker, 1961; Evans and Campbell, 1995; Andriashek and Atkinson, 2007).

85 **2.2 Regional glacial history**

The geomorphic and sedimentological imprints of ice flow within the SWLIS have been well documented, with sediment-landform associations, lithological provenance and till geochemistry being used to reconstruct ice stream catchments and flow orientation (Prest, 1968; Shetsen, 1984; Dyke and Prest, 1987; Evans, 2000; Evans et al., 2008; Ross et al., 2009; Ó Cofaigh et al., 2010; Evans et al., 2012, 2014; Margold et al., 2015b; Atkinson et al., 2016; Utting et al., 2016; Margold et al., 2018; Evans et al., 2020,

90 2021). Within the region, cross-cutting landforms, till lithologies and geochemical signatures document changes in ice flow orientation. Relatively older and overprinted southwesterly ice flows have previously been suggested to be associated with an advancing ice sheet (Ó Cofaigh et al., 2010; Margold et al., 2015b). A dominant southern flow has been attributed to LGM conditions, and a subsequent southeastward and then southwest flow was thought to have operated during ice retreat (Evans, 2000; Evans et al., 2008; Ross et al., 2009; Ó Cofaigh et al., 2010; Evans et al., 2012, 2014; Margold et al., 2015b, a, 2018; Evans et al.,

95 2020, 2021). While these changes in ice stream configuration are prominent in the landform record, they have not been reconstructed in detail for the entire ice sheet sector. Further, the timing of changes in ice sheet dynamics and how they may relate to external climate forcing or internal forcing mechanisms (i.e., glaciological, lithological, and topographic changes) remains largely undetermined.

100 Across the SWLIS, moraines and other ice-marginal landforms relating to ice sheet recession have been the focus of numerous studies (Christiansen, 1979; Dyke and Prest, 1987; Dyke, 2004; Evans et al., 2008; Fisher et al., 2009; Kleman et al., 2010; Evans et al., 2012, 2014). Until recently, the deglacial chronology of the SWLIS was based primarily on radiocarbon data (in compilations by; Dyke, 2004; Dalton et al., 2020), which within the Interior Plains are associated mainly with Quaternary vertebrates and limited by unquantified biases between ice retreat and colonization of the region by plants and animals (c.f. Froese et al., 2019).

105 Furthermore, where infrared/optically stimulated luminescence dating and a small number of [10]Be terrestrial cosmogenic nuclide exposure ages have been used to complement radiocarbon chronologies, significant discrepancies between dating methods across the region meant that the deglacial response of the SWLIS to climate drivers is poorly constrained. Norris et al. (2022) recently addressed these discrepancies by combining pre-existing luminescence and the most viable minimum-limiting radiocarbon dates with new [10]Be exposure ages to establish the timing of SWLIS deglaciation. Within a Bayesian framework, this compilation unified

110 the ages provided by these methods into an internally consistent chronology, which indicates that the SWLIS retreated from its southernmost coalescence with the CIS to its YD position along the Cree Lake Moraine (Fig. 1) in ≤ 2500 yrs (Norris et al., 2022).

3 Methods

3.1 Geomorphological mapping

To create a comprehensive reconstruction of the extent, configuration and dynamics of ice flow as well as the ice-marginal retreat,
115   the glacial geomorphology of the SWLIS was synthesized from pre-existing mapping (Ó Cofaigh et al., 2010; Atkinson et al., 2014; Evans et al., 2016; Norris et al., 2017; Atkinson et al., 2018; Evans et al., 2020). The following landform categories were collated: ice flow parallel lineations (flutings, drumlins, mega-scale glacial lineations (MSGLs), and crag-and-tail features), moraines (major and minor), ice-thrust ridges, crevasse fill ridges, meltwater landforms (major and minor meltwater channels and eskers), palaeo-shorelines and dunes. Geomorphic mapping from LiDAR imagery (5-15 m resolution) (Atkinson et al., 2014, 2018)
120   at a 1:10,000 scale was utilized for Alberta. For all other parts of the study area, geomorphic mapping was completed at a 1:30,000 scale (Norris et al., 2017; this study) and a 1:10,000 scale (Ó Cofaigh et al., 2010; Evans et al., 2016). Due to a lack of accessible LiDAR data within Saskatchewan and northeast British Columbia, mapping was completed from 1-arc second SRTM (~30 m resolution) and ALOS (~30 m resolution) imagery.

3.2 Glacial inversion (flowset classification)

125

We utilized a glacial geomorphological inversion method or flowset approach (see Kleman and Borgström, 1996; Kleman et al., 1997, 2007; Greenwood and Clark, 2009), which formalizes standardized geomorphological mapping techniques (Dyke et al. 1992). The approach uses an accepted understanding of landform genesis to reconstruct ice sheet properties from the mapped characteristics and distribution of glacial geomorphology (Fig. 2). Ice flow patterns were grouped into spatially coherent flowsets
130   based on their morphometry, proximity and parallel concordance and association with other glacial landforms, following the assumption that all lineations in the same flowset should have similar orientations (Clark et al., 1999). Following the procedures adopted by Atkinson et al. (2016), traditional flowset classification was combined with a landsystems approach (see Evans, 2007, 2013). The latter enables landforms and their constituent sediment to be integrated into assemblages related to genetic processes, thereby facilitating a more holistic appreciation of process-form regimes in the assessment of palaeo-ice sheet behaviour (Evans et
135   al., 2008, 2014; Fig. 2).

We synthesized and updated flowsets (mapped and originally presented by Ross et al., 2009; Evans et al., 2016; Norris, 2019; Evans et al., 2020; Atkinson and Utting, 2021) and generated new flowset mapping in regions where no mapping was available (~60% of the SWLIS). Each flowset was then divided into one of six categories: (i) ice stream, (ii) event, (iii) deglacial retreat, (iv)
140   deglacial readvance, (v) palimpsest and (vi) unknown (Table 1). Flowsets were also ordered according to their relative age based on overprinting and crosscutting relations (Kleman et al., 2007; Greenwood and Clark, 2009; Kleman et al., 2010; Hughes et al., 2014) to reconstruct changes in ice sheet dynamics over space and time.

Consistent with previous studies within the Canadian Prairies (e.g. Ross et al., 2009; Ó Cofaigh et al., 2010; Margold et al., 2015b;
145   Stokes et al., 2016), we refer to an 'ice stream' as a corridor within an ice sheet that is flowing relatively faster than the ice surrounding it. We also document switches between periods of rapid ice flow likely driven by internal forcing mechanisms; in such cases, we refer to them as exhibiting 'surge' behaviour (Evans et al., 1999; Clayton et al., 2008; Evans et al., 2020) and classify them as deglacial readvance flowsets.

3.3 Deglacial dynamics

We embedded our reconstruction into the ice margin chronology of Norris *et al.* (2022). This dataset comprises ~150 [10]Be terrestrial cosmogenic exposure ages, infrared/optically stimulated luminescence, and high-quality, minimum-limiting radiocarbon ages. These data were combined within a Bayesian statistical framework to present an internally consistent retreat chronology, which indicates an initial detachment of the SWLIS from its convergence with the CIS occurred at ~15.0 ka BP and the retreat >1200 km to its YD position by ~13.0 ka BP. We combine this chronology with the mapped ice margin positions of Dyke (2004) and Dalton et al. (2020) and present recessional isochrones for the SWLIS.

4 Results

We identify 425 flowsets in the SWLIS landform record (Fig. 3; to view individual flowsets discussed below, see the supplemental .kml file in Google Earth). Approximately 55% of flowsets are categorized as ice stream, 11% as event, 13% as deglacial retreat, 9% as deglacial readvance and 8% as palimpsest flowsets. A small number of flowsets (4%) contained insufficient information to categorize them and are mapped as flowsets of unknown origin. Based on the cross-cutting nature of flowsets, it is evident that ice flow patterns within the SWLIS underwent several macroscale reorganizations (Fig. 3). Below, we present the evolution of ice flow in five phases. While we differentiate our reconstruction into five major snapshots, we note that in many cases, flowsets document a time-transgressive bedform generation (see Greenwood and Clark, 2009) and reflect a rapidly fluctuating ice flow regime. As such, multiple flowsets may depict ice flow in a small region during a single phase. In these cases, the relative timing of flowset evolution is described below and documented in Figure 4.

4.1 Phase 1

Phase 1 documents ice flow from the northeast to the southwest. It comprises 25 flowsets (Fig. 4a) composed of drumlins and flutings. These flowsets are not associated with any ice-marginal landforms. Their imprint is mainly preserved in areas of high ground. They occur as topographically unconstrained southwestward-oriented fast-flow tracts extending >70 km across the Cameron Hills (fs417), Birch Mountains (fs267), Clear Hills (fs300, 348, 349, 353, 355, 358, 362, 369, 379, 388, 390), Stony Mountain (fs123, 130, 157 and 181), Buffalo Head Hills (fs330), and Swan Hills (fs245). Within the eastern portions of the study area, fs10 and 6 record southwestward flow restricted to the valley base, northeast and southwest of Saskatoon and fs 134 and 141 record southwestward flow northeast of Edmonton. Within the Rocky Mountain foothills, southeast to northwest trending ice flow is recorded within the Grande Prairie region (fs 310, 324, 361). These flowsets record northwestward ice flow within the valley base, resulting from flow being deflected by ice draining from the Rocky Mountains.

4.2 Phase 2

Phase 2 documents ice flow from north to south (Fig. 4b) in multiple fast-flow corridors. Within the western portions of the study area during this phase, fs191, 197, 198, 200, 209, 212, 214, 219, 220, 223, 278 and 281 document a series of tributary flows that coalesce in the Athabasca River lowlands as a single flowpath (fs207). These flowsets comprise highly elongate flutes and MSGLs. This single major north-to-south aligned flow bifurcates immediately north of Edmonton. It can be traced over 420 km as an eastern

corridor (f38,51,93,142) and western corridor (fs39, 57, 58, 76, 104, 111, 119, 121, 129, 148, 152, 151, 153, 160, 167, 170, 172, 186, 189, 192, 201,204, 208) to a region of lobate marginal landforms (Lethbridge moraine complex; Stalker, 1962, 1977; Eyles

185 et al., 1999; Evans et al., 2008, 2012). Cordilleran ice draining from the Rocky Mountains is documented by fs55, 59, 68, 70, 75, 80, 84, 87, 90, 91, 168, 170, 174, 190, 213, 242, 248, 262, 265. CIS flows were deflected south by Laurentide ice immediately east of the mountain front.

Within Saskatchewan, north-to-south oriented ice flow is first documented as a small flowset (fs 137) composed of drumlinized

190 terrain located at the southwest boundary of the Canadian Shield. Flow can then be traced to a region of widespread southwest-trending MSGLs (fs42, 49, 54, 61, 62 and 67). The flowpath then extends over 600 km as a succession of seven flowsets (fs12, 16, 18, 19, 24, 30, 42), terminating at a series of lobate marginal moraines and thrust masses on the northern slopes of the Cypress Hills. In several locations, streamlined landforms comprising these flowsets are overprinted by swaths of crevasses fill ridges that are oriented perpendicular to the ice flow direction. South of the Cypress Hills, fs5,7 and 8 document fragmentary evidence of

195 small ice flows that extend towards the ice margin.

4.3 Phase 3

Phase 3 documents ice flow from the northwest to southeast (Fig. 4c). Widespread streamlined subglacial bedforms and glaciotectonic bedrock rafts occur over six broad, northwest to southeasterly ice flow corridors. These corridors separate the

200 widespread hummocky and stagnant ice terrain (in some places locally overprinted by surge-type geomorphic signatures) that characterizes much of the central SWLIS. In several locations, these streamlined zones are overprinted by swaths of crevasses fill ridges that are oriented perpendicular to the ice flow direction. In addition, the lateral boundary of these fast-flow corridors is often demarcated by lateral shear moraines.

205 Within the northern portions of the Churchill River lowlands, fs26, 34, 40, 85, 149 and 150 record ice flow that crosscuts Phase 2 southerly oriented flow. Bedforms that comprise these flowsets are faint due to a surface cover of glaciolacustrine sediment. Thus, the flow direction is difficult to identify based solely on bedform morphology. However, multiple bedrock rafts throughout these flowsets (interpreted as the product of glaciotectonism) indicate ice flow to the southeast. Within the southern portions of the Churchill River lowlands, fs4, 52, 81, 97, 106, 112, 124, 127, 128, 136, 145, 154, 158, 163, 166, 177, 178 record a contemporaneous

210 ice flow that originated northwest of Cold Lake. Areas north and south of the Neutral Hills display similar southeastward-oriented flow as documented by fs28 and 43. This ice flow was subsequently crosscut by a slightly later south-southeast ice flow (fs 2, 3, 9, 25 and 66).

Closer to the western ice margin at this time, ice flow fed lobes in the Calgary (fs72, 74, 82, 92, 99, 102, 116, 121, 131, 144, 148,

215 151, 160, 162, 167, 172, 179, 180, 192, 193, 202 and 208) and Lethbridge regions (fs 11, 13,14,15, 21, 22, 23, 27, 29, 31, 35, 38, 41, 44, 46, 47, 50, 51, 53, 93, 95, 100, 133, 138, 147), recording southwestward ice flow orientations. Within the Grande Prairie region, small ice lobes were fed by Cordilleran (fs 213, 265, 272, 354) and Laurentide ice (fs250, 280, 288, 291, 296, 304, 305, 314, 320, 341, 342, 363). All ice flows during this phase were restricted to the lowland regions, and the regional topography heavily influenced ice flow direction. In several areas, complex overprinting of these wide ice flow corridors occurs, documented by local

220 streamlining and areas of thrust moraines. These are best documented surrounding the Neutral Hills, where small localized surge lobes are identified. These lobes appear to have been sourced from the upland and overprint parts of the regional scale

southwestward flows within the surrounding lowlands (e.g., fs 32,33 48, 60, 79, 88, 98, 110). In several cases these flowset overprint or onlap glaciolacustrine material suggesting that proglacial lakes were present in the landscape during their formation.

4.4 Phase 4

Phase 4 documents southwestward oriented ice flow in the Hay (e.g., fs384, 396, 398, 419, 425), Peace (e.g., 308, 317,326 and 335) and Athabasca (e.g., fs 211,214,219, 222, 227, 236, 244, 254 and 255) river lowlands (Fig. 4d). Evidence for southwesterly ice flow is also recorded on the Birch Mountains (fs 253 and 264), indicating that ice flow within the northernmost portions of the SWLIS was unconstrained by topography. Within the Churchill River lowlands, a southeastward flow is recorded (fs 25, 49, 77, 83, 125 and 146) (Figure 4d). Associated with fs150, two cross-cut lateral shear moraines document a time-transgressive switch from southwest-west to the northeast, northwest-to-southeast and north-to-southeast flow. The cross-cutting relationships exhibited by these landforms suggest they formed as a shifting ice drainage system migrating from west to north source as the ice sheet thinned (i.e. from Phase 3 to 4). A switch from southwestward ice streaming to northwestward ice flow (feeding into the Hay and Peace River ice flows) is also visible north of the Caribou Mountains. Glacial lineations display a migration rather than a simple overprinting, producing a time-transgressive landform assemblage (fs 146 and 125).

4.5 Phase 5

Phase 5 documents the last stages of ice flow to the southwest (Fig. 4e). During this phase, ice flow terminated at the Cree Lake Moraine and Upper Cree Lake Moraine complex. A regionally extensive flowset (fs 164) and a series of smaller discrete retreat and localized readvance flowsets (fs 65, 77, 94, 101, 114, 118, 135, 140 and 161) comprise lineated outcrops of the Canadian Shield.

In addition to flowsets associated with regional deglaciation, this phase documents ice draining radially from several uplands. Flowsets on the Cameron Hills (fs 418, 424), Caribou Mountains (fs 332, 339, 352, 356), Birch Mountains (fs 260 and 275), Clear Hills (fs368, 373, 376) and Swan Hills (fs 274) comprise suites of lineations and ice-marginal channels, eskers and recessional moraines that overprint flowsets documenting regional deglaciation (phase 4 flowsets). These landforms also cross-cut recessional moraines and glaciolacustrine sediments within the surrounding lowlands, suggesting that the lowland regions were ice-free and that proglacial lakes in the area had drained.

5 Dynamic evolution of the SWLIS

To place our ice sheet reconstruction into chronological context, we integrate flowset and ice-marginal geomorphologic mapping with the deglacial chronological synthesis of Norris *et al.* (2022). We combine this ice margin chronology with the mapped ice margin positions of Dyke (2004) and Dalton et al. (2020) and reconstruct ice sheet dynamics and configuration at five phases spanning pre-LGM to early Holocene (Fig. 4).

5.1 Pre-LGM ice flow pattern (Phase 1)

Phase 1 flowsets document the build-up and initial convergence of the CIS and LIS before the LGM. In many cases, flowsets relating to this phase are small and fragmented. To avoid overinterpretation of the geomorphic record, we do not delineate ice stream pathways associated with the pre-LGM ice flow pattern, however in regions where these have previously been identified, we include them in our interpretation (see Fig. 4). Evidence for southwestward fast flow relating to this phase is largely restricted to upland areas (Buffalo Head, Cameron, Clear and Swan Hills and Birch and Stony Mountains) within the central portion of the SWLIS (Fig. 4a). Flowsets on the Cameron Hills are broadly consistent with a region of ice streaming highlighted by Margold et al. (2015a, b) and are interpreted as their 'Cameron Hills Fragments'. Within the eastern part of the study area, southwestward flow is also preserved in the lowland regions surrounding Saskatoon and northeast of Edmonton. Portions of our flowsets in these regions have previously been noted by Ó Cofaigh et al. (2010) and Margold et al. (2015a, b) and, we interpret our flowsets as an extension of their 'Winefred Lake Fragments' and 'Pre 1 Fragments', respectively. Initial convergence between the LIS and CIS is recorded in the Grande Prairie and Calgary regions; here, initial southwestward flows have been progressively deflected northwestward, presumably by ice draining from the Rocky Mountains. Subglacial landforms that comprise flowsets in the Grande Prairie and Calgary regions have been interpreted by Atkinson et al. (2016) to signify synchronous build-up of the CIS and LIS. We support this interpretation and suggest that the ice divide feeding the SWLIS must have been further to the east than when ice divides were at their LGM extent.

Within southern Alberta, we do not document any flowsets relating to this phase, although, overridden glaciotectonic composite ridges have been mapped previously in the region (see Evans et al., 2008, 2012, 2014). These landforms record the proglacial thrusting of pre-LGM fluvial materials and outline the lobate margins of what would become major LGM ice stream tracks (see Evans et al., 2008, 2012, 2014). The configuration of these advance ice lobes also indicates that fast ice flow during ice marginal advance into southern Alberta and Saskatchewan was directed by LIS and CIS convergence.

Little chronological evidence is available relating to the pre-LGM ice sheet evolution within the region. Nevertheless, a southwesterly ice flow orientation is compatible with previous continental reconstructions (Dyke et al., 2002; Batchelor et al., 2019) of pre-LGM buildup following Marine Isotope Stage 3 minimum ice extents. This interpretation also agrees with till geochemical analyses that have documented high concentrations of calcium oxide in tills across southeastern Alberta, which have been linked to a dolomite boulder dispersal train extending over >100 km from central Saskatchewan (Westgate, 1968; Pawluk and Bayrock, 1969).

5.2 LGM ice flow pattern (Phase 2)

During the LGM, flowsets record the development of three north to south-oriented ice streams. This ice flow orientation is broadly consistent with previous regional geomorphic reconstructions (Ross et al., 2009; Ó Cofaigh et al., 2010; Margold et al., 2015b, a, 2018; Evans et al., 2008, 2014) (Fig. 4b) and supports the notion of an extensive ice dome and ice (divide) saddle situated to the north (Dyke and Prest, 1987; Margold et al., 2015b, 2018). Within the eastern portion of the SWLIS, we document the flowpath of the region's most longitudinally extensive ice stream. This ice stream flowpath was first identified as the East Lobe by Shetsen (1984) and was later delineated by Ross (2009) as the Maskwa Corridor and by Ó Cofaigh et al. (2010) as Ice Stream 1 based on mapping of lineations using ~90 m SRTM imagery. To avoid confusion, we herein refer to this ice stream as the Maskwa Ice

Stream (Maskwa IS). The onset zone of the Maskwa IS is cross-cut by later ice flows and is only preserved as a single flowset (fs137). We suggest this flowset marks the distal portion of the convergent flow that straddled the boundary between the crystalline
295 bedrock of the Canadian Shield and sedimentary units occupying the Western Canadian Sedimentary Basin. An onset zone near the Canadian Shield boundary is also supported by regional airborne gamma-ray spectrometry surveys (GSC, 2008; Ross et al., 2009), which document the presence of potassium-rich glacial diamict that has been transported from the Canadian Shield along a north-to-south flowpath that is broadly aligned with fs137.

300 The Maskwa IS extended from its onset zone and terminated on the north slopes of the Cypress Hills >700 km to the south (after Ross et al., 2009; Ó Cofaigh et al., 2010; Margold et al., 2015b). The southernmost advance of the Maskwa IS onto the Cypress Hills likely relates to the upper limit of the Elkwater drift (see Westgate, 1968; Evans et al., 2008). During this time, the Maskwa IS fed two small ice lobes that flowed around the east and west of the Cypress Hills (herein named East and West Cypress Hills fragments) towards the LGM limit of the SWLIS in Montana (Ross et al., 2009; Ó Cofaigh et al., 2010; Evans et al., 2016). These
305 ice lobes probably operated synchronously with tributaries of the Des Moines and James lobes, which collectively drained the southern portion of the Keewatin Ice Dome (Margold et al., 2015a, b, 2018).

Within the Athabasca River lowlands, we document the onset zone of another north-to-south oriented ice stream. Due to its association with previous work further to the south (Prest et al., 1968; Evans et al., 2008; Atkinson et al., 2014), we interpret this
310 as the onset zone of the Central Alberta Ice Stream and High Plains Ice Stream (hereafter CAIS and HPIS). These ice stream flow as a single pathway until they bifurcate immediately north of Edmonton, the western arm becoming the HPIS. The HPIS then coalesced with ice flowing from the CIS to form the Rocky Mountain Foothills Ice Stream (Evans et al., 2008, 2012, 2014). The onset zone of the CAIS/HPIS does not exhibit a zone of convergent flow (i.e. Prest et al., 1968; De Angelis and Kleman, 2008). While it is plausible that the region of convergence was not preserved (e.g., Evans et al., 2014), we instead suggest multiple
315 topographically constrained tributaries rather than a large region of convergent flow-fed fast flow might have been feeding the fast ice flow in the CAIS/HPIS. This is justified by the subtle changes in ice stream orientation recorded within the onset zone and the existence of multiple flowsets (e.g., fs198, 214,219,278 and 281), which are topographically confined immediately north of the ice stream trunk zone.

320 In line with previous reconstructions, we suggest that the SWLIS would have drained via the Maskwa IS, CAIS, HPIS, and Rocky Mountains Foothills IS following the full establishment of the Keewatin Ice Dome and CIS-LIS saddle and thus likely the maximum buildup of the coalescence zone between the CIS-LIS (Dyke and Prest, 1987; Margold et al., 2015b, 2018). Although the absolute age of ice stream initiation is not well constrained, sub-till radiocarbon dates in central Alberta indicate that they must postdate the incursion of the SWLIS into the region after ~25 ka BP (Young et al., 1994).
325

Unlike many parts of the LIS, the LGM ice streams within the SWLIS were largely topographically unconstrained. This is likely a result of the extensive ice thickness in a region immediately southwest of the Keewatin Ice Dome, coupled with the lack of significant subglacial topography over much of the area (Margold et al., 2015b). Although numerical model estimates average LGM ice thicknesses in these regions vary from >1500 to <2000 m (Tarasov et al., 2012; Peltier et al., 2015; Gowan et al., 2016;
330 Lambeck et al., 2017), substantial ice thicknesses are evidenced by observations of glacial isostatic adjustment and postglacial delevelling of proglacially formed palaeo-lake shorelines (e.g. glacial lakes Agassiz and McConnell) (Breckenridge, 2015).

5.3 Rapid downwasting of the LIS and CIS convergence zone (Phase 3)

We map 103 flowsets associated with this ice flow phase that documents a shift from north to south-oriented LGM flows to
335 southeasterly flows. We propose that this change in ice flow orientation is the product of a macroscale switch in the ice dynamics associated with rapid ice sheet thinning and downwasting of the CIS-LIS convergence zone. Southeastward ice flows within the SWLIS were first highlighted by Ross et al. (2009) and Ó Cofaigh et al. (2010), who documented the short-lived IS2 (Buffalo Corridor of Ross et al., 2009) that replaced the north to the south flow of the Maskwa IS. We document these ice streams and map similar southeastward-oriented flows northeast of the Mostoos Hills and north of the Cypress Hills (we herein refer to this collection
340 of ice streams as the IS2 complex).

The change from the topographically unconstrained system of the Maskwa IS, CAIS and HPIS to the topographically constrained southeastward flow of the IS2 complex reflects CIS-LIS saddle collapse and rapid ice downwasting centred in the CIS-LIS convergence zone. Thinning of the CIS-LIS convergence zone is constrained by [10]Be terrestrial cosmogenic exposure dating from the northwest LIS, indicating that the region underwent rapid surface lowering starting at ~14.9-14.3 ka BP (Stoker et al., 2022).
345 In addition, numerical model simulations (Tarasov et al., 2012; Gregoire et al., 2016) suggest that downwasting and separation of the CIS and LIS occurred rapidly, synchronous with initial BA warming (ca. 15 ka BP) (Gregoire et al., 2016; Stoker et al., 2022). We note, however, that during this ice flow phase, an ice divide extending from the Keewatin Ice Dome to the west must have remained (at least partially) active to support easterly flow. Due to substantial ice thinning, this ice divide would no longer have been fed by ice draining across the main ridge of the Rocky Mountains, and so we no longer refer to it as the CIS-LIS saddle.
350 Instead, this divide would have been situated broadly over the Caribou Mountains in northern Alberta (precise position undefined) and is herein referred to as the Plains Ice Divide (after Dyke and Prest, 1987).

Following the initial separation of the LIS and CIS, the SWLIS experienced rapid downwasting and retreat (Norris et al., 2022). Based on the onset locations of multiple south-eastward flowing networks, we agree with the previous suggestions of Ross et al.
355 (2009) and Ó'Cofaigh et al. (2010) who propose that these ice streams would have ceased shortly after the development of an 'ice-free corridor' between the CIS-LIS; otherwise, the onset zones of these ice streams would have had insufficient input from the west to be sustained. The timing of LIS retreat across the Interior Plains suggests that following initial detachment from the CIS, rapid retreat rates continued to characterize SWLIS deglaciation, contemporaneous with BA warming (Norris et al., 2022). Therefore, we suggest that southeasterly-oriented ice flow networks were only in operation for ~500 yrs before they were replaced
360 by westerly flows extending towards the retreating ice margin.

5.4 Deglaciation of the Interior Plains (Phases 4 and 5)

5.4.1 CIS-LIS separation
Our flowset mapping, in combination with previous detailed geomorphic mapping by Evans et al. (2014) suggests that concurrent
365 with initial separation, the lobate margins of the HPIS, CAIS and Maskwa IS experienced a predominantly active recession, at least as far north as the Frank Lake, Lethbridge and Cypress Hills moraines, respectively (Fig. 4c). Interspersed zones of linear hummocky moraine (controlled moraine) and push moraine ridges that comprise these ice-marginal complexes suggest that the ice-stream margin underwent repeated thermal regime switches between polythermal and warm-based conditions during ice retreat (Evans et al., 2014). To the north of the Lethbridge moraine, flowsets that mark the recessional imprint of the HPIS are overridden

370   by thrust moraines and lineations from the CAIS; this landform assemblage supports the previous suggestion of Evans et al. (2008, 2014) of a later stage fast flow event of the CAIS in this region (Fig. 4c). Because these ice streams coalesced and flowed against the regional topographic gradient, ice flow disrupted regional drainage, and a series of small and short-lived ice-dammed proglacial lakes formed at the rapidly retreating margin of the HPIS (Utting and Atkinson, 2019; e.g. glacial lake Cardston, Lethbridge, McLeod; see Bretz, 1943; Horberg, 1952) and the CAIS (e.g. glacial lake Beiseker and Bassano; see Utting and Atkinson, 2019).

375

   The timing of the initial separation of the CIS and the LIS is constrained based on a synthesis of [10]Be terrestrial cosmogenic nuclide exposure, radiocarbon and infrared/optically stimulated luminescence dates that span Alberta-British Columbia (Norris et al., 2022). This chronology suggests that the SWLIS's initial separation began at ~14.9 ka BP (Margold et al., 2019; Norris et al., 2022). Interestingly, [10]Be exposure ages from additional sites in northwestern Alberta and northeastern British Columbia suggest

380   slightly later separation of the two ice sheets at ~13.8 ka BP (Clark et al., 2022b). We do not adjust our timing of initial CIS-LIS separation based on these additional sites but rather continue to use an age of ~14.9 ka BP because this age is supported by three different geochronological techniques displaying internally consistent results (Norris et al., 2022). However, we highlight the inclusion of these additional [10]Be exposure sites from Clark et al. (2022b) would imply that the deglaciation of the SWLIS occurred even more rapidly than previously thought, and thus the ice dynamical switches discussed below would span an even shorter

385   timescale.

5.4.2 Deglaciation of central Alberta and Saskatchewan

   The geomorphic record in central Alberta and Saskatchewan (i.e. northeast of Calgary) suggests deglaciation of the region was the result of widespread stagnation in places punctuated by localized surging (Fig. 5). Within ice stream trunk zones of the CAIS,

390   Maskwa IS, and IS2 and 3, ice sheet stagnation is demarcated by regions of well-preserved elongate lineations (MSGLs, drumlins and flutes) which are overprinted by crevasse fill ridges (Ó Cofaigh et al., 2010; Evans et al., 2016). Crevasse fill ridges are infrequently preserved during active ice margin retreat; thus, their presence in central Alberta and Saskatchewan indicates that ice downwasted in place (Sharp, 1985; Evans, 2007; Evans et al., 2016). Boarding the flowpaths of the above-mentioned ice streams, large swaths of hummocky terrain dominate the landscape. We suggest that ice stagnation here resulted from ice stream switching

395   and isolation of the central portions of the CAIS and Maskwa IS from their accumulation zones by these being tapped by southeastward ice flows (IS2 complex). The short-lived southeastward flows of the IS2 complex would also have ceased following CIS-LIS separation. Thus, the ice margin in this region would no longer have been nourished, and ice stagnation would have been widespread.

400   In some locations, glaciotectonic landforms and small moraine and fluting assemblages locally overprint the palaeo-ice stream footprints (Bretz, 1943; Evans, 2000; Evans et al., 2008, 2014, 2016, 2020; Ó Cofaigh et al., 2010). These landforms attest to the development of small surging ice lobes sourced from upland regions during ice sheet stagnation. In agreement with previous work, we suggest this behaviour was most likely conditioned by the increased availability of subglacial meltwater and the expansion of local proglacial lakes around areas that contained downwasting ice (Evans et al., 2008, 2020). Tightly clustered radiocarbon dates

405   suggest the development of biologically viable conditions over the central SWLIS by ~13.2 ka BP (e.g. Edmonton region; Heintzman et al., 2016; Norris et al., 2022). [10]Be exposure, luminescence, and radiocarbon dates indicate that there were ice-free conditions as far north as the city of Cold Lake by ~13.5 ka BP (Norris et al., 2022). We, therefore, suggest that deglaciation, predominantly via large-scale ice sheet stagnation and downwasting in central Alberta and Saskatchewan occurred rapidly at 13.5 ka. However, we note that portions of the landscape may have remained 'ice-cored' for much longer (see section 6.3.2).

410

5.4.3 Deglaciation of northern Alberta and Saskatchewan

Within the Churchill, Athabasca, Hay and northern portions of the Peace river lowlands, we observe widespread active retreat of the ice margin, fed by southwestward ice streaming of the Hay, Peace and Athabasca ice streams (after Margold et al., 2015b) and southeastward ice streaming of Ice Stream 4/5 (IS4/5) (after Ó Cofaigh et al., 2010). As noted by Margold et al. (2015b), these ice

415   streams were initially unconstrained by regional topography, as evidenced by ice stream flow over the Birch Mountains. However, our flowset mapping suggests that these ice streams were gradually restricted to the southwestward oriented preglacial-valley systems due to ice sheet retreat and thinning. This transition is marked by a series of overprinted flowpaths that document the time-transgressive alteration and increasing influence of topographic controls as the ice sheet thinned.

420   Within all four lowlands, arcuate moraines record ice-marginal recession as a series of discrete lobes (Fig. 4e; Christiansen, 1979; Fisher et al., 2009). Ice retreat in these lowlands led to the development of several large glacial lakes. Within the Peace River lowlands the Peace and Wabasca lakes occupied the region immediately in front of the ice margin on the north and south sides of the Buffalo Head Hills, respectively (Utting and Atkinson, 2019). In the Athabasca and Churchill river lowlands, Glacial Lake McMurray/Meadow occupied the region and the Beaver River Moraine demarcates the position of the ice margin at this time. (Fig.

425   6; Fisher et al., 2009; Anderson, 2012; Utting and Atkinson, 2019). Glacial Lake McMurray/Meadow would have continued to expand until the ice margin was far enough to the northeast to facilitate drainage either into Glacial Lake Agassiz to the southeast (see below) or Glacial Lake McConnell to the north (Fig. 6; Lemmen et al., 1994; Fisher et al., 2009).

[10]Be terrestrial cosmogenic exposure dating suggests that the northern portion of the Athabasca River lowlands (the region

430   surrounding the Clearwater Lower Athabasca Spillway) was ice-free by ~13.0 ka BP (Norris et al., 2022). This suggestion supports luminescence chronologies from the same region that encapsulate a broader but consistent timing of deglaciation (Munyikwa et al., 2017, 2011; Woywitka, 2019). In contrast, radiocarbon dates within the Athabasca River lowlands indicate deglaciation occurred almost 3 ka later, at ~10.7-10.3 ka BP (Dyke, 2004; Fisher et al., 2009; Dalton et al., 2020; Norris et al., 2022). However, when compared to older, more southerly luminescence and radiocarbon dates, these samples provide only minimum-limiting ages

435   for biological productivity in the region (Froese et al., 2019; Norris et al., 2022). In contrast to the Athabasca River lowlands, there are limited chronological constraints within the northern portions of the Peace and Churchill river lowlands. However, based on the geometry of ice-marginal landforms, ice streaming would have been largely synchronous in all three of these lowlands.

5.4.4 Younger Dryas ice flow pattern and deglaciation

440   The YD position of the SWLIS is demarcated by the Cree Lake Moraine and Upper Cree Lake Moraine, which is located immediately up ice flow of the Canadian Shield boundary (Fig. 4e). [10]Be terrestrial cosmogenic exposure dating from two sites located on the crest of the Cree Lake Moraine and Upper Cree Lake Moraine (herein Cree Lake Moraine complex) indicate the region was ice-free at ~12.7 ka BP and 12.3 ka BP, respectively (Norris et al., 2022). Concurrent with ice retreat to the Cree Lake Moraine complex position, Glacial Lake Agassiz occupied the Churchill River lowlands to a maximum elevation recorded by

445   shorelines (Fisher and Smith, 1994; Murton et al., 2010; Breckenridge, 2015; Young et al., 2021). Ice sheet stabilization at the Cree Lake Moraine complex would have permitted drainage of Glacial Lake Agassiz (Fig. 6) to the northwest at some point during the YD stadial (Norris et al., 2021). [10]Be terrestrial cosmogenic exposure dating <50 km northeast of the Cree Lake Moraine complex document deglaciation by 11.2 ka BP, suggesting a stillstand of ~1 ka during the YD. Unlike the lobate, topographically constrained ice flows that occurred in the Churchill, Athabasca and Peace river lowlands as the ice margin retreated onto the

450   Canadian Shield, it was nourished by a regionally extensive (non-ice streaming) fast ice flow event that spread across the region as a broad sheet flow. This change in flow characteristics and the observed change in ice margin retreat rates would have been influenced by the change in the character of the bed (transitioning from the weak, Quaternary sediment and deformable Cretaceous bedrock of the Western Canada Sedimentary Basin to more resistant crystalline lithologies of the Canadian Shield), coupled with the shift to cooler climatic conditions of the YD.

455

In addition to ice flow on the Canadian Shield, we recognise evidence of residual ice caps that persisted after regional deglaciation on the Birch and Caribou Mountains and Cameron and Clear Hills (Fig. 4e). Similar evidence is also documented on the Swan Hills, previously identified by Atkinson (2009) and Atkinson et al., (2016). In these five locations, moraines and meltwater channels that descend into the surrounding lowlands crosscut older flowsets as well as glaciolacustrine material. Based on the overprinting

460   relationships of landforms on these uplands, we suggest that these ice caps were active after their surrounding lowlands were ice-free and that local ice-marginal lakes had drained prior to their advance across the surrounding lowlands (Fig. 6). Although no chronology is available to constrain the timing of their operation, based upon their location relative to regional deglacial isochrones, ice from a dispersal centre on the Swan Hills could not have flowed across ice-free lowlands until after ~13.5 ka BP; similarly, ice on the Birch and Caribou Mountains and, Cameron and Clear Hills, could not have dispersed radially until after ~13 ka BP. Based

465   on this evidence, these upland ice cpas may have been invigorated as a localized response to YD cooling.

6 Discussion

6.1 Timing of ice sheet dynamic changes

Combining our ice dynamic reconstruction with pre-existing chronologies, we reconstruct the behaviour of the SWLIS spanning the LGM to the early Holocene. While switches in ice sheet dynamics and changes in ice-marginal behaviour have previously been

470   recognized for the SWLIS (i.e., Ó Cofaigh et al., 2010; Ross et al., 2009; Margold et al., 2018), the duration over which these dynamic changes occurred and how they relate to climate forcing is less clear.

Integrating our flowset and ice-marginal geomorphic mapping with new deglacial chronologies, our reconstruction depicts three macroscale reorganizations of the ice drainage network followed by rapid ice sheet retreat and widespread stagnation. These

475   changes occurred over a ~2500 yr interval, synchronous with abrupt BA warming (14.7-12.9 ka BP). We, therefore, suggest that ice stream networks documented in the geomorphic record within the SWLIS evolved rapidly and were replaced by subsequent ice flows on centennial timescales. During the LGM, the SWLIS drained via three large north-to-south oriented ice streams that were unconstrained by the regional topography. South-eastward flowing, topographically constrained ice streams subsequently replaced these unconstrained ice streams during a macroscale switch in ice sheet dynamics. We suggest this switch from

480   unconstrained to topographically constrained ice flows occurred contemporaneously with rapid ice sheet thinning at 14.9-14.3 ka BP (Stoker et al., 2022). South-eastward ice streaming would only have been sustained for a short period while the Plains Ice Divide remained active to support flow from the northwest to the southeast (Ross et al., 2009; Ó Cofaigh et al., 2010). Following complete CIS-LIS separation and the development of an 'ice-free corridor', south-eastward ice flows would have ceased. In the central portions of the SWLIS, we observe widespread ice sheet downwasting and effective collapse associated with the shutdown

485   of south-eastward flows and the isolation of this region. Within the northern portions of the SWLIS, south-eastward ice stream corridors were replaced by south-westward oriented ice streams that fed the rapidly retreating ice margin between 14.5-13 ka BP

(Norris et al., 2022). As the ice margin reaches the Canadian Shield boundary at ~13 ka BP, we observe a ~1500 yr ice marginal standstill of the SWLIS. This standstill occurred contemporaneously with YD (12.9-11.7 ka BP) cooling.

490   **6.2 Drivers of ice sheet dynamics**

Comparing our reconstruction with climatic driving forces, macroscale reorganization and deglaciation of the SWLIS occurred synchronously with climatic warming during the BA interval. We propose that ice sheet thinning during this interval would have exerted a major control on the SWLIS dynamics. First, our reconstruction documents an initial switch in ice flow orientation from large topographically unconstrained ice streams that flowed north to south (CAIS, HPIS, Maskwa IS) to southeastward ice

495   streaming (IS 2 complex), the orientation of which was controlled by the regional subglacial topography of the region and fed by Plains Ice Divide. In agreement with previous work, we suggest that ice sheet thinning likely impeded north-to-south ice flow due to there being a lack of adequate ice thickness to sustain topographically unconstrained flows (Ross et al., 2009; Ó Cofaigh et al., 2010). A second macroscale ice sheet reorganization within the northern portions of the SWLIS was characterized by a switch to southwestward ice streaming (Hay, Peace, and Athabasca river IS). We suggest this switch was driven by further ice sheet thinning,

500   the shutdown of the Plains Ice Divide and the complete separation of the LIS and CIS. As the two ice sheets thinned and separated, there would have been inadequate ice input from the northwest to feed ice streaming to the southeast, and thus these ice flowpaths would have been replaced by ice streams that travelled through the Hay, Peace and Athabasca river lowlands fed solely by the Keewatin Ice Dome.

505   In both cases, ice stream dynamics were likely driven by ice sheet thinning and changing ice divide configuration. However, we propose that these changes alone would not have caused these dramatic switches in ice stream orientation. Instead, these macroscale changes in ice sheet dynamics observed in the SWLIS are moderated by the region's subglacial topography (i.e. preglacial valley network). As the ice sheet thinned, the subglacial topography in the region ultimately controlled the direction of ice stream switching. As such, this control, internal to the ice sheet system, influenced the wider response of the SWLIS to BA warming.

510

Our reconstruction also depicts a distinct change in the dynamics of the SWLIS during the YD. During this period of climatic cooling, we observe a slowdown in the ice sheet retreat rate and a widespread standstill of the SWLIS marked by the formation of the regionally extensive Cree Lake Moraine complex. At the same time, we record a switch from topographically constrained ice streaming in the Hay, Peace, Athabasca, and Churchill river lowlands to a regionally extensive and unconstrained (non-ice

515   streaming) sheet flow that fed the ice margin at its Cree Lake Moraine position. While it is highly likely that these dynamics are influenced by the external climate forcing of the YD, we suggest that the regions' underlying lithology and topography moderated the ice sheets' response to climate forcing. Interestingly, these changes in ice flow behaviour and regional ice margin standstill occur at the transition from the soft (deformable) sediment-covered Western Canadian Sedimentary Basin to the hard (rigid) bed of the Canadian Shield. We propose that this change in lithology would have resulted in an increase in bed strength that would have

520   increased frictional resistance at the ice-bed interface resulting in a decrease in ice velocity and, thus, potentially a slowing of the rate of ice sheet retreat (Bradwell et al., 2019). This pattern is analogous to changes observed in the northern portions of the British Irish Ice Sheet (Bradwell et al., 2019), which highlighted the importance of bedrock lithology in changing ice sheet dynamics. In this case, a transition from a relatively soft to hard bed resulted in a reduction in ice retreat rates and changes in ice stream behaviour. The simultaneous change in lithology and climate experienced by the SWLIS is unique, however, and may

525   therefore help explain why this sector of the LIS has such a marked response to YD cooling in comparison to other portions of the western Laurentide margin (e.g., Gauthier et al., 2022; Reyes et al., 2022).

The dynamics we highlight above attest to the importance of considering glaciological, lithological and topographic factors in addition to external climate forcing when assessing ice sheet dynamic evolution over time. The changes in ice stream orientation,

530 ice margin stagnation and localized surging highlighted in our reconstruction have not yet been well replicated by the existing numerical ice sheet reconstructions for the SWLIS (e.g., Tarasov et al., 2012). Quantifying and incorporating the effects of internal as well as external controls into numerical model reconstructions of the SWLIS should be a key area for future work to address.

6.3 The geomorphic imprint of abrupt climate change

535 In addition to the observed changes in ice flow direction, our geomorphic reconstruction also provides insight into the pattern and mechanism of ice recession. We observe a geomorphic imprint characterized by a period of active recession, widespread ice sheet stagnation punctuated by localized surging and then a return to widespread active recession. The spatial variability in landforms diagnostic of these changes is best described as three zones. A southern 'Outer Deglacial Zone' encompasses the region between the LGM ice margin position and its retreat as far north as Red Deer (~52°N), an 'Intermediate Deglacial Zone'

540 encompasses the central regions of Alberta and Saskatchewan spanning from Red Deer to Cold Lake (~55°N) and an 'Inner Deglacial Zone' that spans the most northerly portion of the SWLIS and includes the region from Cold Lake to the Cree Lake Moraine complex. The juxtaposition of these three zones is likely the result of macroscale ice flow reorganizations that occurred during ice sheet thinning and deglaciation.

545 **6.3.1 Outer Deglacial Zone**

At the southern limits of the SWLIS, recessional push moraines are common across the landscape, most prominently the Lethbridge Moraine and the recessional moraines that overly the northern face of Cypress Hills (Westgate, 1968; Stalker, 1977; Kulig, 1996; Evans et al., 2008, 2012, 2014; Fig 5 and 6a). Such landforms represent active recession, which appears to have characterized the margin of the HPIS, CAIS, and Maskwa IS until they had retreated to the region north of Red Deer (Fig. 4d). Outside of these ice

550 stream tracks, active recession is marked by arcuate zones of 'aligned hummocks, ponds and ice-walled lake plains' (controlled moraine) diagnostic of warm and polythermal ice-marginal conditions (identified and mapped by Evans et al., 2014; Fig. 3). This region also contains very limited glaciolacustrine sediments and landforms, which has previously been interpreted to be indicative of small, shallow and very short-lived proglacial lakes (Utting and Atkinson, 2019). We suggest this is the result of rapid active-ice sheet recession, which inhibited long-lived, widespread lake formation.

555

6.3.2 Intermediate Deglacial zone

The geomorphic record in central Alberta and Saskatchewan (i.e., north of Red Deer) contains a geomorphic record of widespread stagnation punctuated by localised surging (Fig. 5). Within the ice stream trunk zones of the CAIS and Maskwa IS and the south-westward IS2 complex that crosses the region, ice sheet stagnation is demarcated by regions of well-preserved lineations (MSGLs,

560 drumlins and flutes), which are overprinted by crevasse fill ridges (Ó Cofaigh et al., 2010). Bordering the flowpaths of these ice streams, large swaths of inter-ice stream moraine containing hummocky terrain dominate the landscape. In some locations, glaciotectonic landforms and small localized arcuate moraine and fluting assemblages that overprint the palaeo-ice stream tracks are interpreted as the product of local late-stage ice surging (Bretz, 1943; Evans, 2000; Evans et al., 2008; Ó Cofaigh et al., 2010; Evans et al., 2014, 2016; Atkinson et al., 2016; Evans et al., 2020). We suggest that local scale surging that punctuated widespread

565 stagnation

was most likely conditioned by the increased availability of subglacial meltwater and the expansion of local proglacial lakes around areas that contained downwasting ice (Evans et al., 2008, 2020).

570 We propose that the intermediate deglacial zone results from an 'ice sheet collapse' (ice sheet sector isolation, stagnation and downwasting) caused by ice stream switching and subsequent shutdown. This geomorphic signature was previously highlighted by Ó Cofaigh et al. (2010) and Ross et al. (2009) and we support the notion that this macroscale ice flow reorganization would have caused stagnation in higher topographic regions. These regions would have become disconnected from the ice sheet accumulation zone as ice flows shifted and began to flow in a southeast direction in topographically confined low-elevation areas. Following rapid ice sheet thinning, these southeast flowpaths would also have ceased, and ice would have downwasted in place,

575 resulting in ice stagnation, including within the former ice stream flowpaths. In some locations, small local surge lobes would have occurred, overprinting the underlying geomorphology.

Although widespread ice sheet stagnation and downwasting (initial ice sheet collapse) would have been rapid, the landscape may have remained 'ice-cored' for several thousand years. In such regions, the thinning of the ice sheet would have allowed permafrost

580 to aggrade beneath it and persist in the ice-cored terrain. Therefore, many regions of ice-cored hummocky terrain southwest of the Cree Lake Moraine, while formed during rapid ice downwasting, would have continued to be modified by thermokarst processes related to thawing of buried glacier ice into the Early Holocene. For example, in central Alberta in the Beaver Hills/ Cooking Lake region (20 km east of Edmonton), Emerson (1983) suggest glacial ice melt and permafrost thaw continued into the early Holocene and persisted until 9 ka BP based on radiocarbon ages from postglacial freshwater molluscs.

585

6.3.3 Inner Deglacial zone

Further north, within the Churchill, Athabasca and Peace river lowlands, inset push moraines, eskers, and meltwater channels dominate the landscape. These landforms document active retreat of the Hay, Peace and Athabasca River ice streams and IS 4/5 (Fig. 3). In these regions, hummocky terrain is scarce and mostly restricted to upland regions (e.g., the Caribou and Birch

590 Mountains). Active ice retreat can be traced northeast, following the long axis of each valley as far north as the Canadian Shield boundary. The ice sheet retreat slowed to a standstill at this location to form the regionally extensive Cree Lake Moraine complex.

The marked change in deglacial behaviour observed across the SWLIS demonstrate the instability of a terrestrially terminating ice margin under rapid climatic warming. The behaviour of the 'Intermediate Deglacial Zone' was the result of macroscale ice stream

595 reorganization that isolated a large portion of the SWLIS and forced an effective collapse in this region. This ice stream response was triggered by the rapid thinning of the CIS-LIS convergence zone, collapse of the CIS-LIS saddle and final shutdown of the Plains Ice Divide and thus highlights how the ice sheet, through changes in the ice flow regime, can be highly sensitive to rapid climatic change. Although the response of the SWLIS to climatic change is complex and non-linear, we suggest that its geomorphic imprint identified here not be unique and propose that the juxtaposition of regions of rapid ice marginal retreat and ice sheet

600 disintegration and downwasting may be a valuable indicator of terrestrial ice sheet collapse.

6.4 Comparison to other ice sheets dynamics

The documented changes within the SWLIS provide valuable insight into the dynamics of ice streams in a region associated with a terrestrially terminating ice sheet margin during a period of rapid climate change. Despite its much larger scale, the behaviour of

605 the SWLIS exhibits similarities to the deglacial changes observed within the interior portions of the last British Irish Ice Sheet

(Greenwood and Clark, 2009; Davies et al., 2019; Clark et al., 2022a) and the (Late Weichselian) Svalbard-Barents Sea Ice Sheet (Landvik et al., 2014). These ice sheets exhibited relatively rapid, major changes in ice sheet and ice stream dynamics during a single glaciation. In all three cases, at maximum ice sheet conditions, the ice sheet dynamics were primarily controlled by external climatic forcings, such as changes in global temperatures and regional precipitation patterns, and were less sensitive to internal

610 controls, such as topography or lithological variations. However, as noted by Davies et al. (2019) as the ice sheet thickness and volume decreased, the role of lithological and topographic controls became increasingly significant, modifying the macroscale changes in ice flow dynamics that occurred in response to the external climatic forcing. We suggest that macroscale reorganizations of ice stream drainage networks during the last deglaciation were commonplace and that both internal and external controls play a critical role in controlling the rapid and large-scale changes in ice flow that occur during periods of deglaciation (Greenwood and

615 Clark, 2009; Ross et al., 2009; Ó Cofaigh et al., 2010; Landvik et al., 2014; Margold et al., 2015b; Davies et al., 2019). As palaeo-ice streams have been shown to be useful analogs for understanding the potential response of modern ice streams to ongoing climatic warming, the results of our study highlight the importance of incorporating both internal and external controls when assessing ice flow dynamics and ice sheet stability.

7 Conclusion

620 Using glacial geomorphological inversion methods (flowsets) in combination with a recently compiled regional chronological sythesis, we reconstruct the ice flow and ice marginal retreat dynamics of the SWLIS into five snapshots of ice sheet behaviour spanning pre–LGM to early Holocene. Our reconstruction depicts a complex pattern of ice stream behaviour characterized by three macroscale reorganizations of the ice drainage network followed by regional deglaciation synchronous with abrupt warming during the BA interstadial. Initial westward flow, most probably indicates of a developing ice stream network during the advance to the

625 LGM. During the LGM southward ice streaming within the Maskwa IS, CAIS and HPIS reflects ice flow unconstrained by topography. Following this, at 15 ka BP, a major switch in the ice sheets dynamics occurred, involving south-eastward flow of the IS2 complex constrained by regional subglacial topography. A second major switch in the ice sheets dynamics, subsequently initiated southwesterly ice flow in the Hay, Peace, Athabasca, and Churchill river lowlands, reflecting the full decoupling of the LIS and CIS, prior to 14 ka BP. During the YD, rates of ice sheet retreat then slowed. At this time the ice sheet margin was located

630 north of the Canadian Shield boundary and ice flow continued to be sourced from the northeast. Resulting from these phases of ice sheet dynamics we observe a zonation of ice marginal geomorphology within the SWLIS, that demarcates active ice margin recession followed by punctuated ice sheet stagnation and downwasting (terrestrial ice sheet collapse). We attribute these, macroscale changes in ice flow geometry and the associated deglacial behaviour to external climatic forcing during the BA and YD. We highlight also the concordant role of internal (glaciological, lithological and topographic) controls in influencing how an

635 ice sheet response to external climate forcing. Significantly, our reconstruction demonstrates that rapid macroscale reorganizations in ice sheet flow patterns are not restricted to marine-based ice marginal settings, but also occur in regions associated with terrestrially terminating margins.

Data availability. The data referred to in this paper is provided within the tables and figures in the main text and in the supplementary materials related to this article are available in the Supplement and at

640 https://figshare.com/s/4270b557926dd0806938. LiDAR DEMs were provided by the Government of Alberta (2017). LiDAR Data Archives. These data were provided under license and with project specific data sharing agreements by the Archaeological Survey of Alberta, Culture, Multiculturalism, and the Status of Women. Edmonton, Alberta via geodiscoveralberta@gov.ab.ca through https://geodiscover.alberta.ca/ geoportal/#searchPanel.

The Cryosphere
Discussions

Open Access

EGU

Supplement. The supplement related to this article is available online at: https://figshare.com/s/4270b557926dd0806938

655 **References**

Alley, R. B. and Bindschadler, R. A.: The West Antarctic Ice Sheet: behavior and environmentEdited by Richard B. Alley & Robert A. Bindschadler Antarctic Research Series volume 77, American Geophysical Union, Washington (2001). 294 pages. Price (65 AGU members 45.50). ISBN 0 87590957 4, Antarct. Sci., 13, 221–222, https://doi.org/10.1017/s0954102001220306, 2001.

Alley, R. B., Clark, P. U., Huybrechts, P., and Joughin, I.: Ice-sheet and sea-level changes, Science, 310, 456–460,
660 https://doi.org/10.1126/science.1114613, 2005.

Anderson, T. W.: Evidence from Nipawin Bay in Frobisher Lake, Saskatchewan, for three highstand and three lowstand lake phases between 9 and 10 (10.1 and 11.5 cal) ka BP, Quat. Int., 260, 66–75, https://doi.org/10.1016/j.quaint.2011.09.021, 2012.

Andriashek, L. D. and Atkinson, N.: Buried channels and glacial-drift aquifers in the Fort McMurray region, Northeast Alberta, Earth Sciences Report 2007-01, Alberta Geological Survey, Alberta Energy Utilities Board, 160, 2007.

665 Andriashek, L. D. and Barendregt, R. W.: Evidence for Early Pleistocene glaciation from borecore stratigraphy in north-central Alberta, Canada, Can. J. Earth Sci., 54, 445–460, https://doi.org/10.1139/cjes-2016-0175, 2017.

Atkinson, Utting, and Pawley: An update to the glacial landforms map of Alberta, Alberta Geological Survey, 2018.

Atkinson, N.: Surficial Geology and Quaternary History of the High PrairieArea (NTS 83N/SE), 2009.

Atkinson, N. and Utting, D.: Glacial Flowlines of Alberta, 2021.

670 Atkinson, N., Utting, D. J., and Pawley, S. M.: Glacial landforms of Alberta, Alberta Geological Survey, AER/AGS Map 604, 2014.

Atkinson, N., Pawley, S., and Utting, D. J.: Flow-pattern evolution of the Laurentide and Cordilleran ice sheets across west-central Alberta, Canada: implications for ice sheet growth, retreat and dynamics during the last glacial cycle, J. Quat. Sci., 31, 753–768, https://doi.org/10.1002/jqs.2901, 2016.

675 Banks, J. and Harris, N. B.: Geothermal potential of Foreland Basins: A case study from the Western Canadian Sedimentary Basin, Geothermics, 76, 74–92, https://doi.org/10.1016/j.geothermics.2018.06.004, 2018.

Batchelor, C. L., Margold, M., Krapp, M., Murton, D. K., Dalton, A. S., Gibbard, P. L., Stokes, C. R., Murton, J. B., and Manica, A.: The configuration of Northern Hemisphere ice sheets through the Quaternary, Nat. Commun., 10, 3713, https://doi.org/10.1038/s41467-019-11601-2, 2019.

680 Bradwell, T., Small, D., Fabel, D., Smedley, R. K., Clark, C. D., Saher, M. H., Callard, S. L., Chiverrell, R. C., Dove, D., Moreton, S. G., Roberts, D. H., Duller, G. A. T., and Ó Cofaigh, C.: Ice-stream demise dynamically conditioned by trough shape and bed strength, Sci. Adv., 5, eaau1380, https://doi.org/10.1126/sciadv.aau1380, 2019.

Breckenridge, A.: The Tintah-Campbell gap and implications for glacial Lake Agassiz drainage during the Younger Dryas cold interval, Quat. Sci. Rev., 117, 124–134, https://doi.org/10.1016/j.quascirev.2015.04.009, 2015.

685 Bretz, J. H.: Keewatin end moraines in Alberta, Canada, Geol. Soc. Am. Bull., 54, 31–52, https://doi.org/10.1130/gsab-54-31, 1943.

Carlson, A. E. and Clark, P. U.: Ice sheet sources of sea level rise and freshwater discharge during the last deglaciation, Rev. Geophys., 50, https://doi.org/10.1029/2011rg000371, 2012.

Christiansen, E. A.: The Wisconsinan deglaciation, of southern Saskatchewan and adjacent areas, Can. J. Earth Sci., 16, 913–938, 690 https://doi.org/10.1139/e79-079, 1979.

Clark, C. D., Ely, J. C., Hindmarsh, R. C. A., Bradley, S., Ignéczi, A., Fabel, D., Ó Cofaigh, C., Chiverrell, R. C., Scourse, J., Benetti, S., Bradwell, T., Evans, D. J. A., Roberts, D. H., Burke, M., Callard, S. L., Medialdea, A., Saher, M., Small, D., Smedley, R. K., Gasson, E., Gregoire, L., Gandy, N., Hughes, A. L. C., Ballantyne, C., Bateman, M. D., Bigg, G. R., Doole, J., Dove, D., Duller, G. A. T., Jenkins, G. T. H., Livingstone, S. L., McCarron, S., Moreton, S., Pollard, D., Praeg, D., Sejrup, H. P., Van 695 Landeghem, K. J. J., and Wilson, P.: Growth and retreat of the last British–Irish Ice Sheet, 31 000 to 15 000 years ago: the BRITICE-CHRONO reconstruction, Boreas, 51, 699–758, https://doi.org/10.1111/bor.12594, 2022a.

Clark, J., Carlson, A. E., Reyes, A. V., Carlson, E. C. B., Guillaume, L., Milne, G. A., Tarasov, L., Caffee, M., Wilcken, K., and Rood, D. H.: The age of the opening of the Ice-Free Corridor and implications for the peopling of the Americas, Proc. Natl. Acad. Sci. U. S. A., 119, e2118558119, https://doi.org/10.1073/pnas.2118558119, 2022b.

700 Clark, P. U.: Unstable behavior of the Laurentide ice sheet over deforming sediment and its implications for climate change, Quat. Res., 41, 19–25, https://doi.org/10.1006/qres.1994.1002, 1994.

Clark, P. U., Alley, R. B., and Pollard, D.: Northern hemisphere ice-sheet influences on global climate change, Science, 286, 1104–1111, https://doi.org/10.1126/science.286.5442.1104, 1999.

Clark, P. U., Dyke, A. S., Shakun, J. D., Carlson, A. E., Clark, J., Wohlfarth, B., Mitrovica, J. X., Hostetler, S. W., and McCabe, 705 A. M.: The Last Glacial Maximum, Science, 325, 710–714, https://doi.org/10.1126/science.1172873, 2009.

Clayton, L., Teller, J. T., and Attig, J. W.: Surging of the southwestern part of the Laurentide Ice Sheet, Boreas, 14, 235–241, https://doi.org/10.1111/j.1502-3885.1985.tb00726.x, 2008.

Dalton, A. S., Margold, M., Stokes, C. R., and Tarasov, L.: An updated radiocarbon-based ice margin chronology for the last deglaciation of the North American Ice Sheet Complex, Quat. Sci. Rev., 2020.

710 Davies, B. J., Livingstone, S. J., Roberts, D. H., Evans, D. J. A., Gheorghiu, D. M., and Ó Cofaigh, C.: Dynamic ice stream retreat in the central sector of the last British-Irish Ice Sheet, Quat. Sci. Rev., 225, 105989, https://doi.org/10.1016/j.quascirev.2019.105989, 2019.

De Angelis, H. and Kleman, J.: Palaeo-ice-stream onsets: examples from the north-eastern Laurentide Ice Sheet, Earth Surf. Process., 33, 560–572, https://doi.org/10.1002/esp.1663, 2008.

715 Dyke, A. S.: An outline of North American deglaciation with emphasis on central and northern Canada, in: Quaternary Glaciations-Extent and Chronology - Part II: North America, Elsevier, 373–424, https://doi.org/10.1016/s1571-0866(04)80209-4, 2004.

Dyke, A. S. and Prest, V. K.: Late Wisconsinan and Holocene history of the Laurentide Ice Sheet, Géogr. phys. quat., 41, 237–263, https://doi.org/10.7202/032681ar, 1987.

Dyke, A. S., Andrews, J. T., Clark, P. U., England, J. H., Miller, G. H., Shaw, J., and Veillette, J. J.: The Laurentide and Innuitian 720 ice sheets during the Last Glacial Maximum, Quat. Sci. Rev., 21, 9–31, https://doi.org/10.1016/s0277-3791(01)00095-6, 2002.

Emerson, D.: Late glacial molluscs from the Cooking Lake moraine, Alberta, Canada, Can. J. Earth Sci., 20, 160–162, https://doi.org/10.1139/e83-014, 1983.

Evans, D. J. A.: Quaternary geology and geomorphology of the Dinosaur Provincial Park area and surrounding plains, Alberta, Canada: the identification of former glacial lobes, drainage diversions and meltwater flood tracks, Quat. Sci. Rev., 19, 931–958, https://doi.org/10.1016/s0277-3791(99)00029-3, 2000.

Evans, D. J. A.: Glacial Landsystems, in: Glacier Science and Environmental Change, Blackwell Publishing, Malden, MA, USA, 83–88, https://doi.org/10.1002/9780470750636.ch18, 2007.

Evans, D. J. A.: GLACIAL LANDFORMS | Glacial Landsystems, in: Encyclopedia of Quaternary Science, Elsevier, 813–824, https://doi.org/10.1016/b978-0-444-53643-3.00069-8, 2013.

Evans, D. J. A. and Campbell, I. A.: Quaternary stratigraphy of the buried valleys of the lower Red Deer River, Alberta, Canada, J. Quat. Sci., 10, 123–148, https://doi.org/10.1002/jqs.3390100204, 1995.

Evans, D. J. A., Lemmen, D. S., and Rea, B. R.: Glacial landsystems of the southwest Laurentide Ice Sheet: modern Icelandic analogues, J. Quat. Sci., 14, 673–691, https://doi.org/10.1002/(sici)1099-1417(199912)14:7<673::aid-jqs467>3.0.co;2-#, 1999.

Evans, D. J. A., Clark, C. D., and Rea, B. R.: Landform and sediment imprints of fast glacier flow in the southwest Laurentide Ice Sheet, J. Quat. Sci., 23, 249–272, https://doi.org/10.1002/jqs.1141, 2008.

Evans, D. J. A., Hiemstra, J. F., Boston, C. M., Leighton, I., Cofaigh, C. Ó., and Rea, B. R.: Till stratigraphy and sedimentology at the margins of terrestrially terminating ice streams: case study of the western Canadian prairies and high plains, Quat. Sci. Rev., 46, 80–125, https://doi.org/10.1016/j.quascirev.2012.04.028, 2012.

Evans, D. J. A., Young, N. J. P., and Ó Cofaigh, C.: Glacial geomorphology of terrestrial-terminating fast flow lobes/ice stream margins in the southwest Laurentide Ice Sheet, Geomorphology (Amst.), 204, 86–113, https://doi.org/10.1016/j.geomorph.2013.07.031, 2014.

Evans, D. J. A., Storrar, R. D., and Rea, B. R.: Crevasse-squeeze ridge corridors: Diagnostic features of late-stage palaeo-ice stream activity, Geomorphology , 258, 40–50, https://doi.org/10.1016/j.geomorph.2016.01.017, 2016.

Evans, D. J. A., Atkinson, N., and Phillips, E.: Glacial geomorphology of the Neutral Hills Uplands, southeast Alberta, Canada: The process-form imprints of dynamic ice streams and surging ice lobes, Geomorphology (Amst.), 350, 106910, https://doi.org/10.1016/j.geomorph.2019.106910, 2020.

Evans, D. J. A., Phillips, E. R., and Atkinson, N.: Glacitectonic rafts and their role in the generation of Quaternary subglacial bedforms and deposits, Quat. Res., 104, 101–135, https://doi.org/10.1017/qua.2021.11, 2021.

Eyles, N., Boyce, J. I., and Barendregt, R. W.: Hummocky moraine: sedimentary record of stagnant Laurentide Ice Sheet lobes resting on soft beds, Sediment. Geol., 123, 163–174, https://doi.org/10.1016/s0037-0738(98)00129-8, 1999.

Fenton, M. M., Waters, E. J., Pawley, S. M., Atkinson, N., Utting, D. J., and McKay, K.: Surficial geology of Alberta. Alberta Geological Survey, Alberta Geological Survey, AER/AGS Map 601, 2013.

Fisher, T. G. and Smith, D. G.: Glacial Lake Agassiz: Its northwest maximum extent and outlet in Saskatchewan (Emerson Phase), Quat. Sci. Rev., 13, 845–858, https://doi.org/10.1016/0277-3791(94)90005-1, 1994.

Fisher, T. G., Waterson, N., Lowell, T. V., and Hajdas, I.: Deglaciation ages and meltwater routing in the Fort McMurray region, northeastern Alberta and northwestern Saskatchewan, Canada, Quat. Sci. Rev., 28, 1608–1624, https://doi.org/10.1016/j.quascirev.2009.02.003, 2009.

Froese, D. F., Young, J. M., Norris, S. L., and Margold, M.: Availability and viability of the ice-free corridor and pacific coast routes for the peopling of the Americas, SAA Archaeological Record, 2019.

Gauthier, M. S., Breckenridge, A., and Hodder, T. J.: Patterns of ice recession and ice stream activity for the MIS 2 Laurentide Ice Sheet in Manitoba, Canada, Boreas, 51, 274–298, https://doi.org/10.1111/bor.12571, 2022.

Gowan, E. J., Tregoning, P., Purcell, A., Montillet, J.-P., and McClusky, S.: A model of the western Laurentide Ice Sheet, using observations of glacial isostatic adjustment, Quat. Sci. Rev., 139, 1–16, https://doi.org/10.1016/j.quascirev.2016.03.003, 2016.

Greenwood, S. L. and Clark, C. D.: Reconstructing the last Irish Ice Sheet 1: changing flow geometries and ice flow dynamics deciphered from the glacial landform record, Quat. Sci. Rev., 28, 3085–3100, https://doi.org/10.1016/j.quascirev.2009.09.008, 2009.

Gregoire, L. J., Otto-Bliesner, B., Valdes, P. J., and Ivanovic, R.: Abrupt Bølling warming and ice saddle collapse contributions to the Meltwater Pulse 1a rapid sea level rise, Geophys. Res. Lett., 43, 9130–9137, https://doi.org/10.1002/2016GL070356, 2016.

GSC: Geoscience Data Repository. Natural Resources Canada, Ottawa, 2008.

770 Heintzman, P. D., Froese, D., Ives, J. W., Soares, A. E. R., Zazula, G. D., Letts, B., Andrews, T. D., Driver, J. C., Hall, E., Hare, P. G., Jass, C. N., MacKay, G., Southon, J. R., Stiller, M., Woywitka, R., Suchard, M. A., and Shapiro, B.: Bison phylogeography constrains dispersal and viability of the Ice Free Corridor in western Canada, Proc. Natl. Acad. Sci. U. S. A., 113, 8057–8063, https://doi.org/10.1073/pnas.1601077113, 2016.

Horberg, L.: Pleistocene drift sheets in the Lethbridge region, Alberta, Canada, J. Geol., 60, 303–330, 775 https://doi.org/10.1086/625981, 1952.

Hughes, A. L. C., Clark, C. D., and Jordan, C. J.: Flow-pattern evolution of the last British Ice Sheet, Quat. Sci. Rev., 89, 148–168, https://doi.org/10.1016/j.quascirev.2014.02.002, 2014.

Kleman, J. and Borgström, I.: Reconstruction of palaeo-ice sheets: The use of geomorphological data, Earth Surf. Process., 21, 893–909, https://doi.org/10.1002/(sici)1096-9837(199610)21:10<893::aid-esp620>3.0.co;2-u, 1996.

780 Kleman, J., Hättestrand, C., Borgström, I., and Stroeven, A.: Fennoscandian palaeoglaciology reconstructed using a glacial geological inversion model, J. Glaciol., 43, 283–299, https://doi.org/10.1017/s0022143000003233, 1997.

Kleman, J., Httestrand, C., Stroeven, A. P., Jansson, K. N., De Angelis, H., and Borgstrm, I.: Reconstruction of palaeo-ice sheets - inversion of their glacial geomorphological record, in: Glacier Science and Environmental Change, Blackwell Publishing, Malden, MA, USA, 192–198, https://doi.org/10.1002/9780470750636.ch38, 2007.

785 Kleman, J., Jansson, K., De Angelis, H., Stroeven, A. P., Hättestrand, C., Alm, G., and Glasser, N.: North American Ice Sheet build-up during the last glacial cycle, 115–21kyr, Quat. Sci. Rev., 29, 2036–2051, https://doi.org/10.1016/j.quascirev.2010.04.021, 2010.

Kulig, J. J.: The glaciation of the Cypress Hills of Alberta and Saskatchewan and its regional implications, Quat. Int., 32, 53–77, https://doi.org/10.1016/1040-6182(95)00059-3, 1996.

790 Lambeck, K., Purcell, A., and Zhao, S.: The North American Late Wisconsin ice sheet and mantle viscosity from glacial rebound analyses, Quat. Sci. Rev., 158, 172–210, https://doi.org/10.1016/j.quascirev.2016.11.033, 2017.

Landvik, J. Y., Alexanderson, H., Henriksen, M., and Ingólfsson, Ó.: Landscape imprints of changing glacial regimes during ice-sheet build-up and decay: a conceptual model from Svalbard, Quat. Sci. Rev., 92, 258–268, https://doi.org/10.1016/j.quascirev.2013.11.023, 2014.

795 Lemmen, D. S., Duk-Rodkin, A., and Bednarski, J. M.: Late glacial drainage systems along the northwestern margin of the Laurentide Ice Sheet, Quat. Sci. Rev., 13, 805–828, https://doi.org/10.1016/0277-3791(94)90003-5, 1994.

Margold, M., Stokes, C. R., Clark, C. D., and Kleman, J.: Ice streams in the Laurentide Ice Sheet: a new mapping inventory, J. Maps, 11, 380–395, https://doi.org/10.1080/17445647.2014.912036, 2015a.

Margold, M., Stokes, C. R., and Clark, C. D.: Ice streams in the Laurentide Ice Sheet: Identification, characteristics and comparison 800 to modern ice sheets, Earth-Sci. Rev., 2015b.

Margold, M., Stokes, C. R., and Clark, C. D.: Reconciling records of ice streaming and ice margin retreat to produce a palaeogeographic reconstruction of the deglaciation of the Laurentide Ice Sheet, Quat. Sci. Rev., 2018.

Margold, M., Gosse, J. C., Hidy, A. J., Woywitka, R. J., Young, J. M., and Froese, D.: Beryllium-10 dating of the Foothills Erratics Train in Alberta, Canada, indicates detachment of the Laurentide Ice Sheet from the Rocky Mountains at ~15 ka, Quat. Res., 92, 805 469–482, https://doi.org/10.1017/qua.2019.10, 2019.

Mossop, G. D. and Shetsen, I.: Geological atlas of the Western Canada Sedimentary Basin; Canadian Society of Petroleum Geologists, Canadian Society of Petroleum Geologists and Alberta Research Council, 2012.

Munyikwa, K., Feathers, J. K., Rittenour, T. M., and Shrimpton, H. K.: Constraining the Late Wisconsinan retreat of the Laurentide ice sheet from western Canada using luminescence ages from postglacial aeolian dunes, Quat. Geochronol., 6, 407–422, 810 https://doi.org/10.1016/j.quageo.2011.03.010, 2011.

Munyikwa, K., Rittenour, T. M., and Feathers, J. K.: Temporal constraints for the Late Wisconsinan deglaciation of western Canada using eolian dune luminescence chronologies from Alberta, Palaeogeogr. Palaeoclimatol. Palaeoecol., 470, 147–165, https://doi.org/10.1016/j.palaeo.2016.12.034, 2017.

815 Murton, J. B., Bateman, M. D., Dallimore, S. R., Teller, J. T., and Yang, Z.: Identification of Younger Dryas outburst flood path from Lake Agassiz to the Arctic Ocean, Nature, 464, 740–743, https://doi.org/10.1038/nature08954, 2010.

Norris, S., Tarasov, L., Monteath, A. J., Gosse, J. C., Hidy, A. J., Margold, M., and Froese, D. G.: Rapid retreat of the southwestern Laurentide Ice Sheet during the Bølling-Allerød interval, Geology, https://doi.org/10.1130/g49493.1, 2022.

Norris, S. L.: Glacial Flowlines in the Lower Athabasca and Clearwater Region Alberta and Saskatchewan, 2019.

Norris, S. L., Margold, M., and Froese, D. G.: Glacial landforms of northwest Saskatchewan, J. Maps, 2017.

820 Norris, S. L., Garcia-Castellanos, D., Jansen, J. D., Carling, P. A., Margold, M., Woywitka, R. J., and Froese, D. G.: Catastrophic drainage from the northwestern outlet of glacial Lake Agassiz during the Younger Dryas, Geophysical, 2021.

Ó Cofaigh, C., Evans, D. J. A., and Smith, I. R.: Large-scale reorganization and sedimentation of terrestrial ice streams during late Wisconsinan Laurentide Ice Sheet deglaciation, Geol. Soc. Am. Bull., 122, 743–756, https://doi.org/10.1130/b26476.1, 2010.

Pattyn, F., Ritz, C., Hanna, E., Asay-Davis, X., DeConto, R., Durand, G., Favier, L., Fettweis, X., Goelzer, H., Golledge, N. R., 825 Kuipers Munneke, P., Lenaerts, J. T. M., Nowicki, S., Payne, A. J., Robinson, A., Seroussi, H., Trusel, L. D., and van den Broeke, M.: The Greenland and Antarctic ice sheets under 1.5 °C global warming, Nat. Clim. Chang., 8, 1053–1061, https://doi.org/10.1038/s41558-018-0305-8, 2018.

Pawluk, S. and Bayrock, L. A.: Some characteristics and physical properties of Alberta tills, Research Council of Alberta, 1969.

Peltier, W. R., Argus, D. F., and Drummond, R.: Space geodesy constrains ice age terminal deglaciation: The global ICE-6G_C 830 (VM5a) model, Journal of Geophysical Research: Solid Earth, 120, 450–487, 2015.

Prest, V. K.: Nomenclature of moraines and ice-flow features as applied to the glacial map of Canada, Department of Energy, Mines and Resources, 1968.

Prest, V. K., Grant, D. R., and Rampton, V. N.: Glacial Map of Canada, in: Geological Survey of Canada, Ottawa, 1968.

Rasmussen, S. O., Bigler, M., Blockley, S. P., Blunier, T., Buchardt, S. L., Clausen, H. B., Cvijanovic, I., Dahl-Jensen, D., Johnsen, 835 S. J., Fischer, H., Gkinis, V., Guillevic, M., Hoek, W. Z., Lowe, J. J., Pedro, J. B., Popp, T., Seierstad, I. K., Steffensen, J. P., Svensson, A. M., Vallelonga, P., Vinther, B. M., Walker, M. J. C., Wheatley, J. J., and Winstrup, M.: A stratigraphic framework for abrupt climatic changes during the Last Glacial period based on three synchronized Greenland ice-core records: refining and extending the INTIMATE event stratigraphy, Quat. Sci. Rev., 106, 14–28, https://doi.org/10.1016/j.quascirev.2014.09.007, 2014.

Reyes, A. V., Carlson, A. E., Milne, G. A., Tarasov, L., Reimink, J. R., and Caffee, M. W.: Revised chronology of northwest 840 Laurentide ice-sheet deglaciation from 10Be exposure ages on boulder erratics, Quat. Sci. Rev., 277, 107369, https://doi.org/10.1016/j.quascirev.2021.107369, 2022.

Rignot, E. and Kanagaratnam, P.: Changes in the velocity structure of the Greenland Ice Sheet, Science, 311, 986–990, https://doi.org/10.1126/science.1121381, 2006.

Rignot, E. and Thomas, R. H.: Mass balance of polar ice sheets, Science, 297, 1502–1506, 845 https://doi.org/10.1126/science.1073888, 2002.

Rignot, E., Bamber, J. L., van den Broeke, M. R., Davis, C., Li, Y., van de Berg, W. J., and van Meijgaard, E.: Recent Antarctic ice mass loss from radar interferometry and regional climate modelling, Nat. Geosci., 1, 106–110, https://doi.org/10.1038/ngeo102, 2008.

Rignot, E., Velicogna, I., van den Broeke, M. R., Monaghan, A., and Lenaerts, J. T. M.: Acceleration of the contribution of the 850 Greenland and Antarctic ice sheets to sea level rise, Geophys. Res. Lett., 38, https://doi.org/10.1029/2011gl046583, 2011.

Ross, M., Campbell, J. E., Parent, M., and Adams, R. S.: Palaeo-ice streams and the subglacial landscape mosaic of the North American mid-continental prairies, Boreas, 38, 421–439, https://doi.org/10.1111/j.1502-3885.2009.00082.x, 2009.

Sharp, M.: "crevasse-fill" ridges—A landform type characteristic of surging glaciers?, Geogr. Ann. Ser. A. Phys. Geogr., 67, 213–220, https://doi.org/10.1080/04353676.1985.11880147, 1985.

855   Shepherd, A.: Mass balance of the Antarctic Ice Sheet from 1992 to 2017, Nature, 556, 219–222, 2018.

Shetsen, I.: Application of till pebble lithology to the differentiation of glacial lobes in southern Alberta, Can. J. Earth Sci., 21, 920–933, https://doi.org/10.1139/e84-097, 1984.

Stalker, A. M.: Buried valleys in cetnral and southern Alberta, Geological Survey of Canada Paper, 1961.

Stalker, A. M.: Surficial geology, Lethbridge (east half), Geoglogical Survey of Canada, Ottawa, 1962.

860   Stalker, A. M.: Indications of Wisconsin and earlier man from the southwest Canadian prairies, Ann. N. Y. Acad. Sci., 288, 119–136, https://doi.org/10.1111/j.1749-6632.1977.tb33606.x, 1977.

Stoker, B. J., Margold, M., Gosse, J. C., Hidy, A. J., Monteath, A. J., Young, J. M., Gandy, N., Gregoire, L. J., Norris, S. L., and Froese, D.: The collapse of the Laurentide-Cordilleran ice saddle and early opening of the Mackenzie Valley, Northwest Territories, constrained by [10]Be exposure dating, , https://doi.org/10.5194/tc-2022-120, 2022.

865   Stokes, C. R. and Clark, C. D.: Geomorphological criteria for identifying Pleistocene ice streams, Ann. Glaciol., 28, 67–74, https://doi.org/10.3189/172756499781821625, 1999.

Stokes, C. R., Margold, M., Clark, C. D., and Tarasov, L.: Ice stream activity scaled to ice sheet volume during Laurentide Ice Sheet deglaciation, Nature, 530, 322–326, https://doi.org/10.1038/nature16947, 2016.

Tarasov, L., Dyke, A. S., Neal, R. M., and Peltier, W. R.: A data-calibrated distribution of deglacial chronologies for the North
870   American ice complex from glaciological modeling, Earth Planet. Sci. Lett., 315–316, 30–40, https://doi.org/10.1016/j.epsl.2011.09.010, 2012.

Utting, D. J. and Atkinson, N.: Proglacial lakes and the retreat pattern of the southwest Laurentide Ice Sheet across Alberta, Canada, Quat. Sci. Rev., 2019.

Utting, D. J., Atkinson, N., Pawley, S., and Livingstone, S. J.: Reconstructing the confluence zone between Laurentide and
875   Cordilleran ice sheets along the Rocky Mountain Foothills, south-west Alberta, J. Quat. Sci., 31, 769–787, https://doi.org/10.1002/jqs.2903, 2016.

Westgate, J. A.: Surficial geology of the Foremost-Cypress Hills region, Alberta, 1968.

Woywitka, R.: Geoarchaeology of the mineable oil sands region, Northeastern Alberta, Canada, 2019.

Young, J. M., Reyes, A. V., and Froese, D. G.: Assessing the ages of the Moorhead and Emerson phases of glacial Lake Agassiz
880   and their temporal connection to the Younger Dryas cold reversal, Quat. Sci. Rev., 251, 106714, https://doi.org/10.1016/j.quascirev.2020.106714, 2021.

Young, R. R., Burns, J. A., Smith, D. G., Arnold, L. D., and Rains, R. B.: A single, late Wisconsin, Laurentide glaciation, Edmonton area and southwestern Alberta, Geology, 22, 683, https://doi.org/10.1130/0091-7613(1994)022<0683:aslwlg>2.3.co;2, 1994.
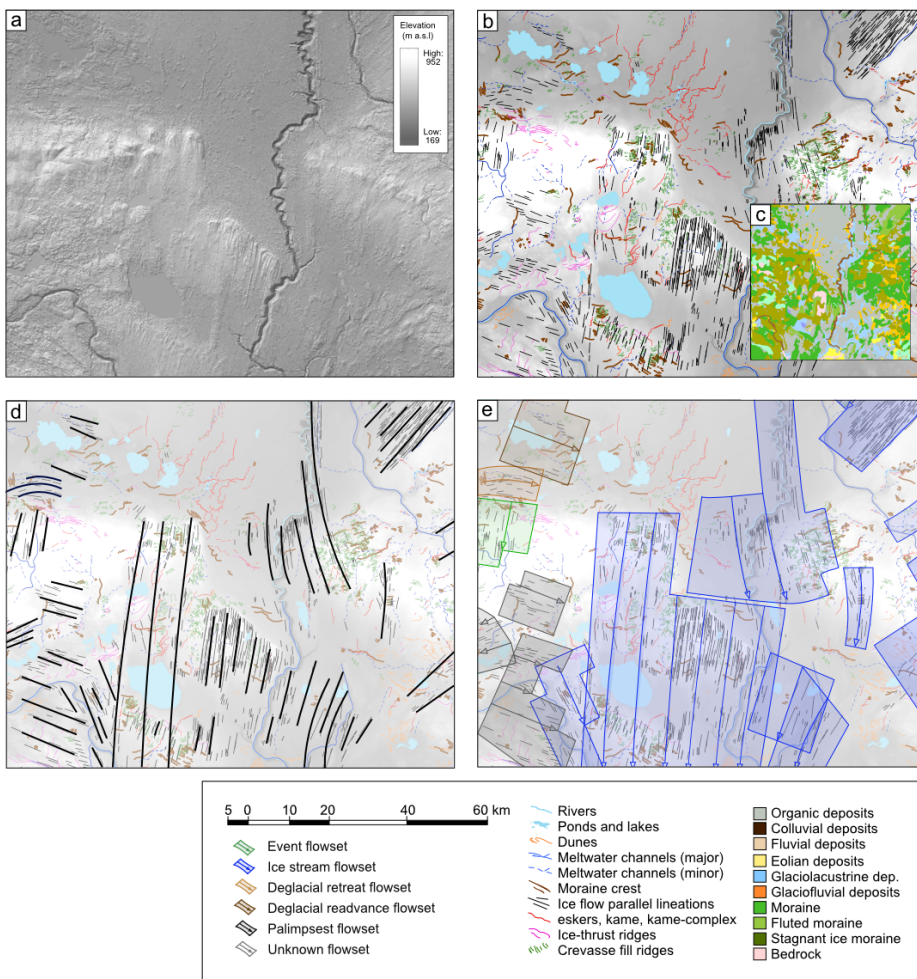
885

890
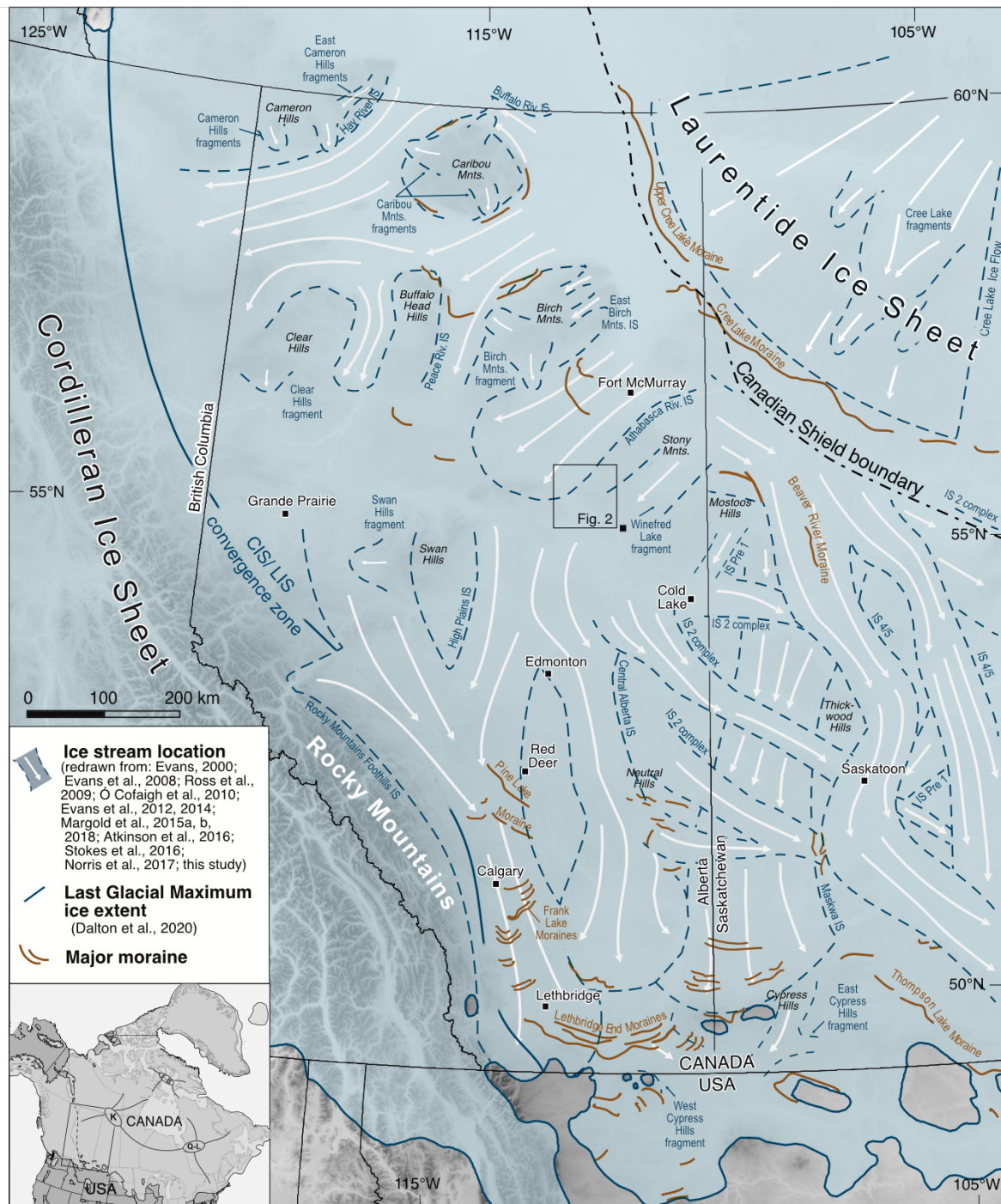
895

Figure 1: Regional ice-flow imprint of the southwestern sector of the Laurentide Ice Sheet.

Figure 2: Classification of glacial geomorphology into flowsets. (a) Shuttle Radar Topography Mission (SRTM) imagery displaying the onset zone of the Central Alberta Ice Stream. **(b)** Area of corresponding geomorphological mapping (from Atkinson et al., 2018) and, **(c)** surficial geological units (from Fenton et al., 2013)**(d).** Simplification of geomorphic mapping and surficial geological units into 'flowlines' **(e)** Classification of flowlines into individual flowsets as either 'ice stream', 'deglacial retreat', "deglacial readvance' 'event' 'palimpsest' or 'unknown. See Figure 1 for the location of Figure 2 panel.

25
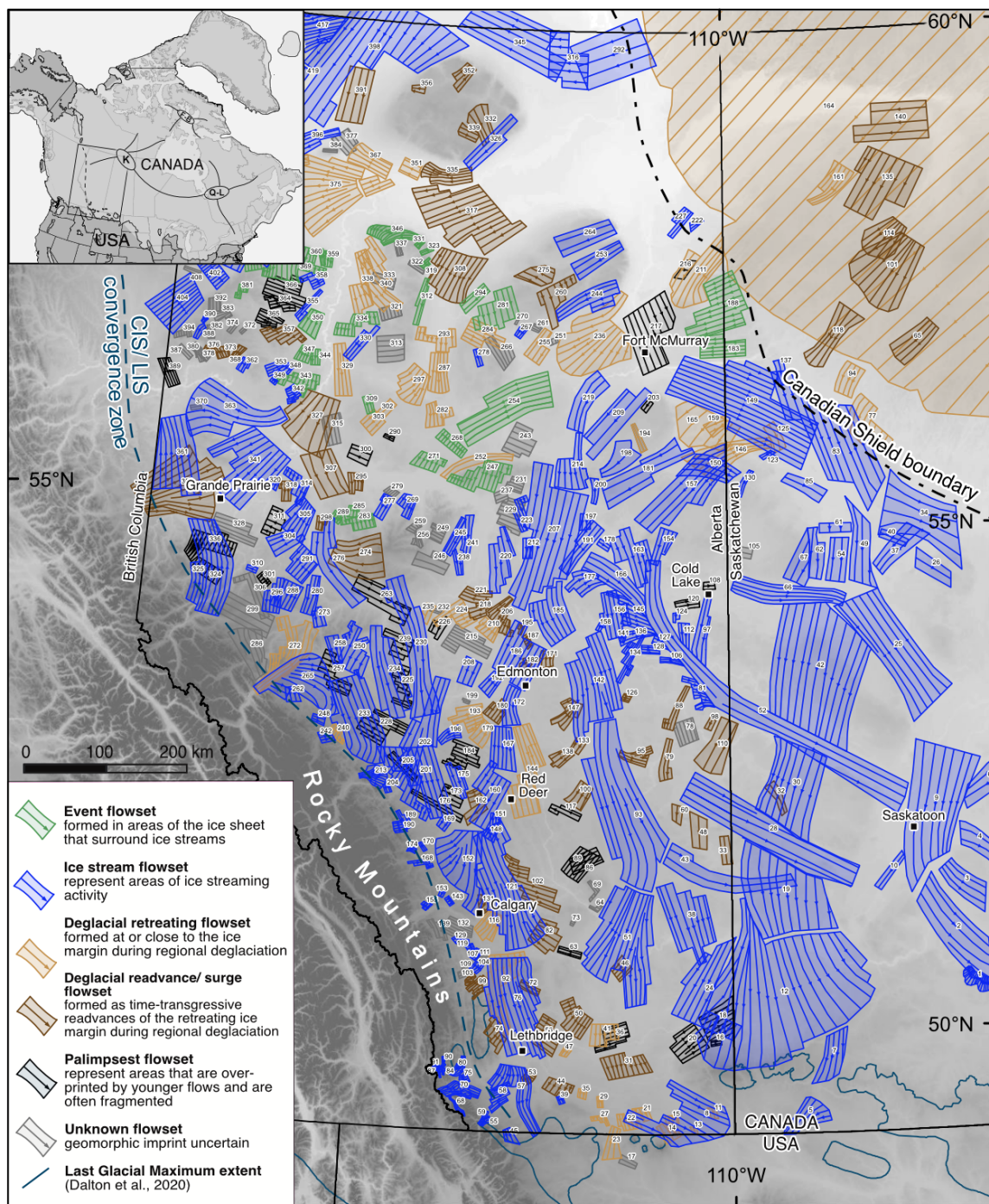
Figure 3: Flowset map of the southwestern Laurentide Ice Sheet (available as a supplementary .kml file). Flowset configuration reflects a highly dynamic system of fast flow caused by multiple reconfigurations in ice sheet drainage.

910

915

920
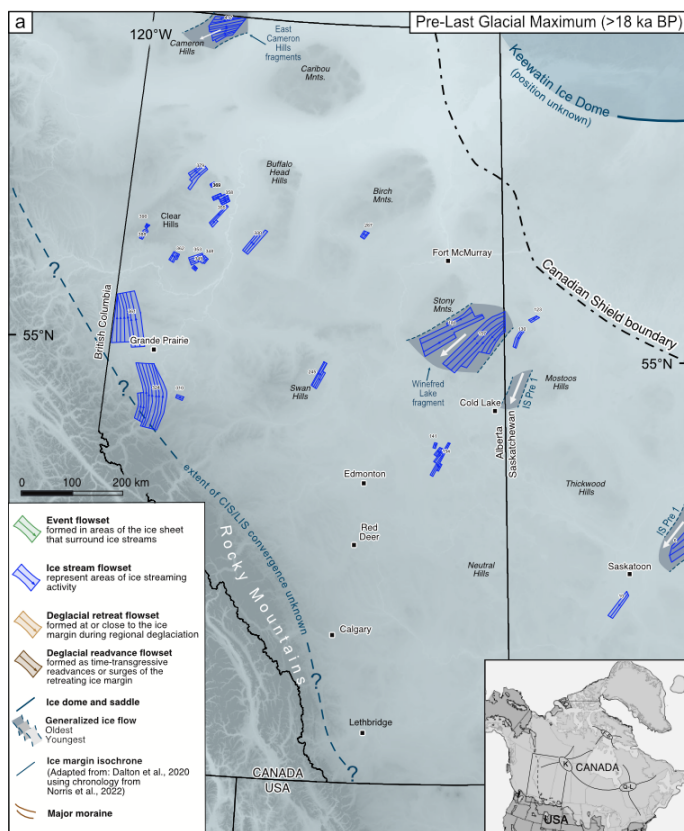
Figure 4: Deglacial ice flow dynamics of the southwestern Laurentide Ice Sheet. This reconstruction presents a comprehensive synthesis, collating pre-existing ice stream mapping with ice streams presented in this study. Timing of ice retreat and associated ice flow reorganizations are constrained using the deglacial chronology of Norris et al. (2022).

925

*Note Figure 4 is a five-panel figure; Panel (a) is above and panels (b-e) are below.*
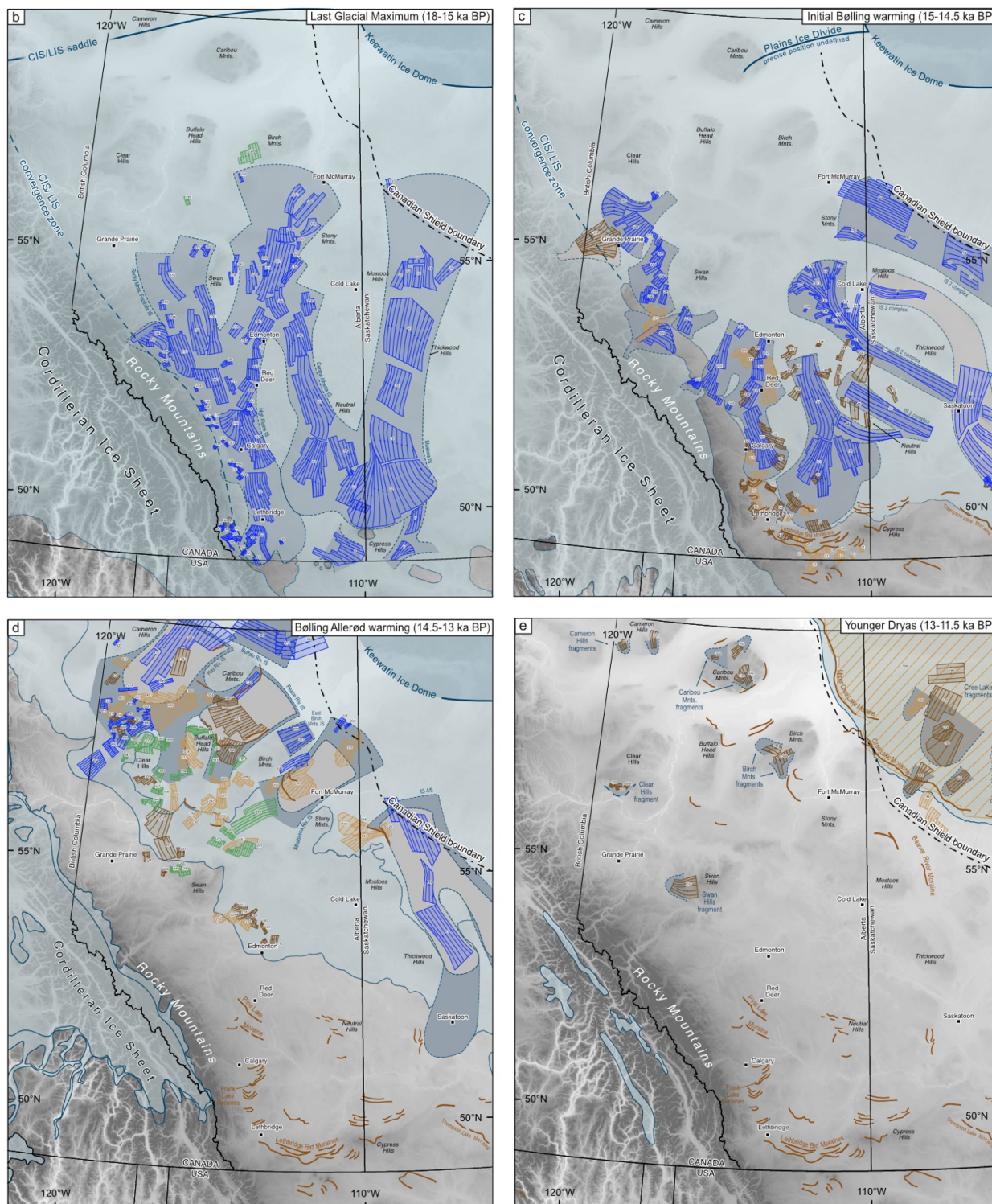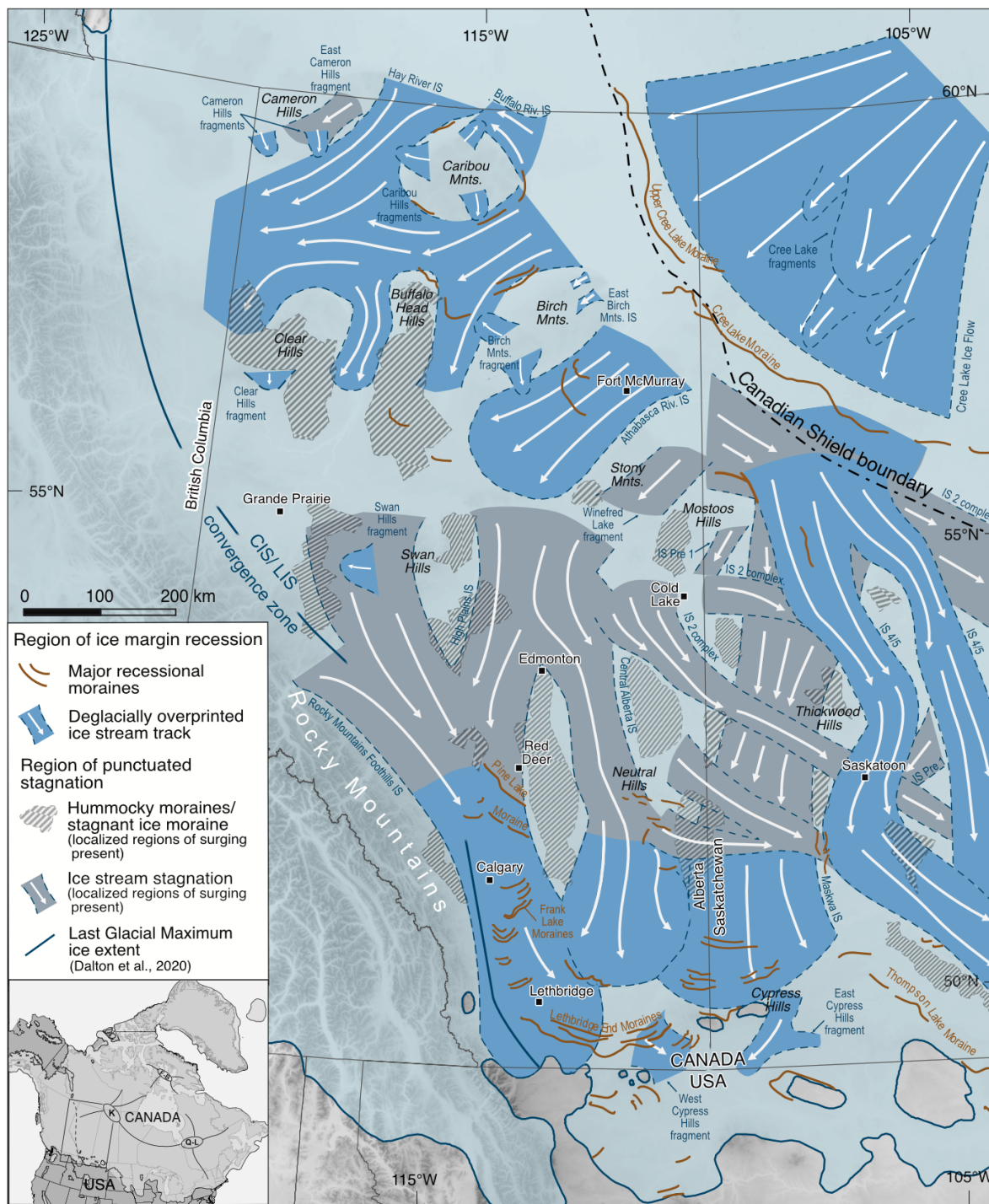
Figure 5: Regional geomorphic imprint of the distribution of ice sheet active retreat and punctuated stagnation across the southwestern Laurentide Ice Sheet.
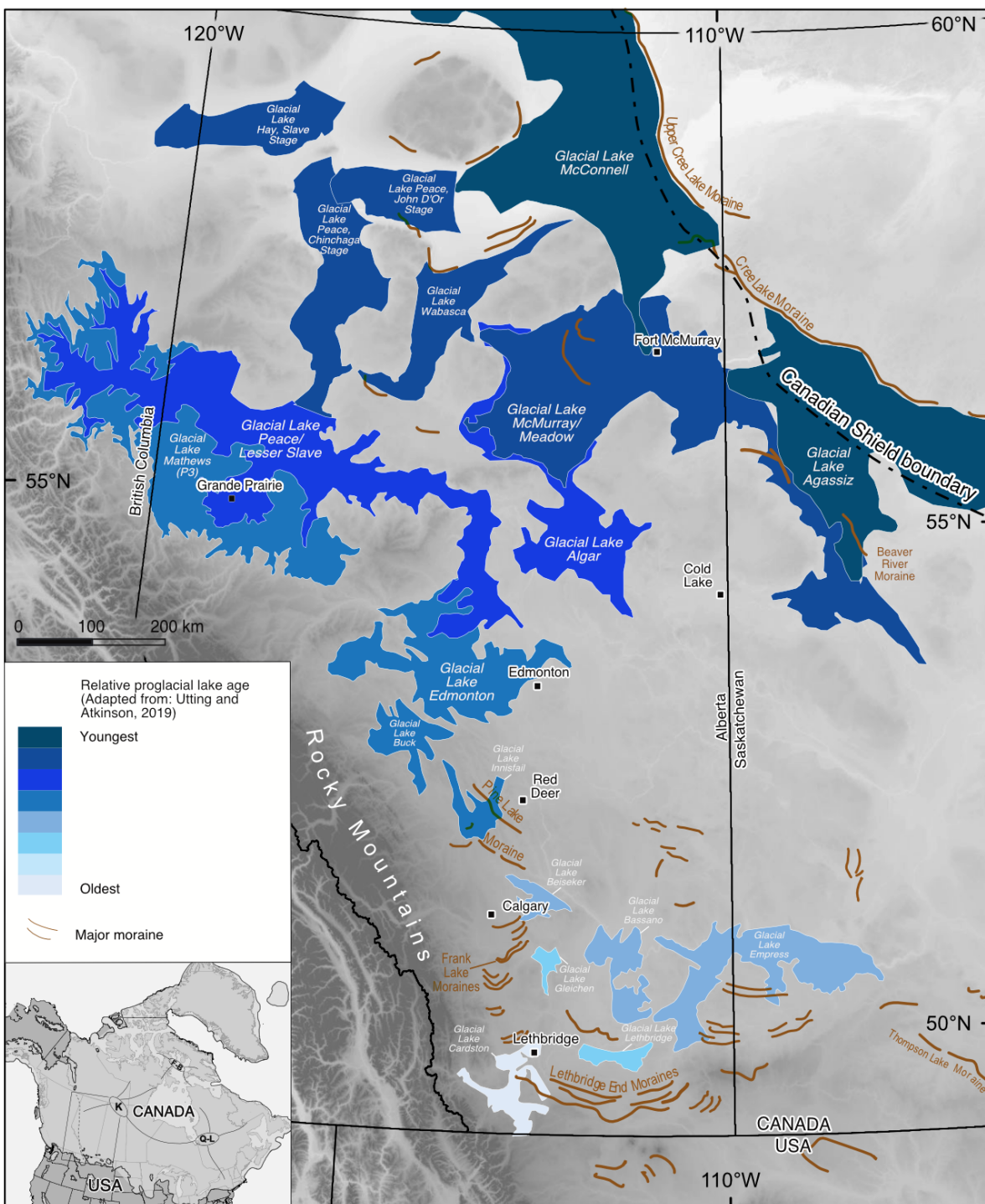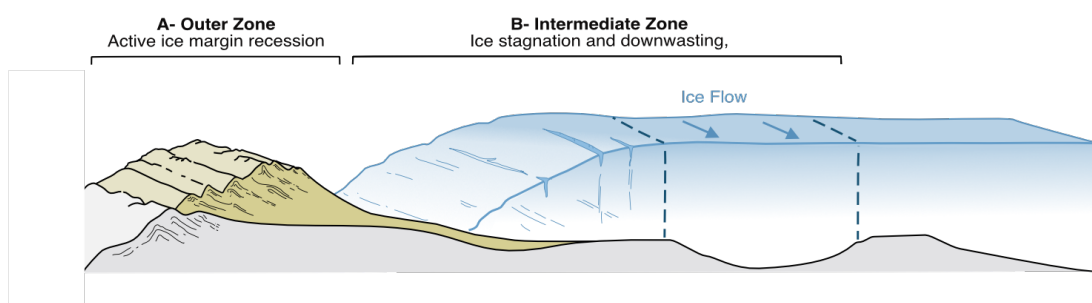
Figure 6: Distribution of reconstructed proglacial lakes associated with the retreat of the southwestern Laurentide Ice Sheet, classified by relative age.
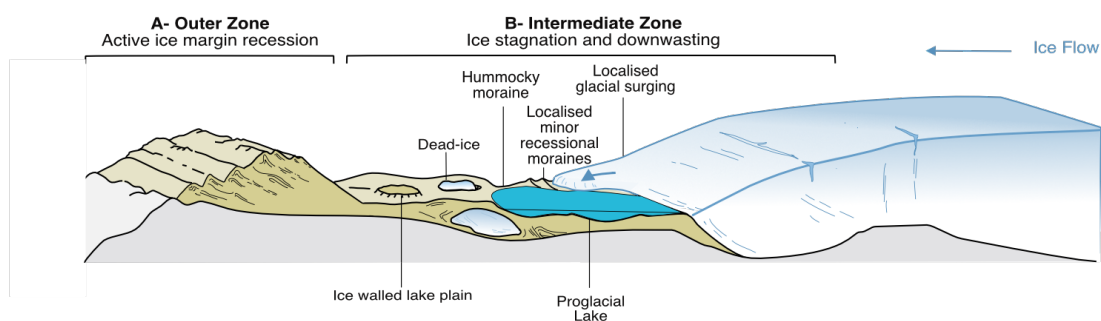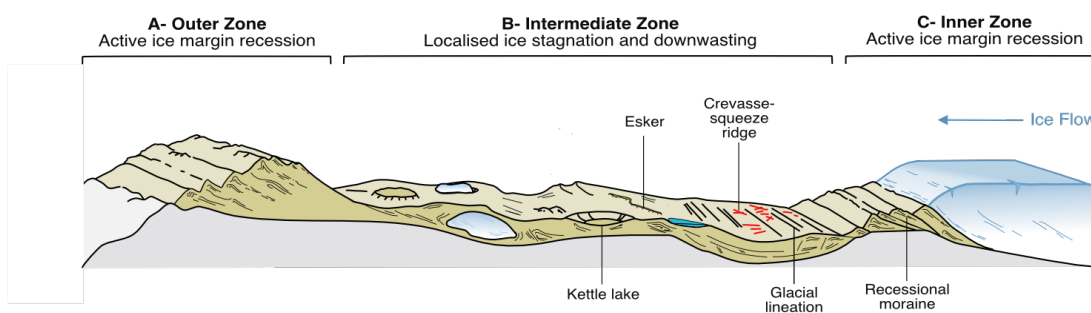
935

a INITIAL ICE MARGIN RETREAT
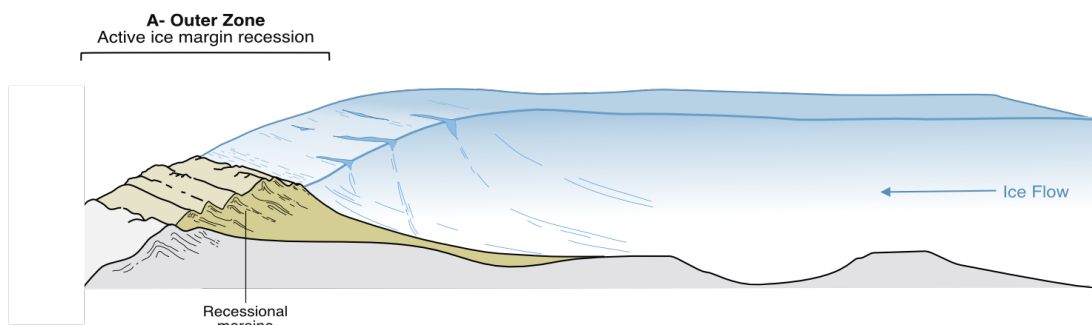
b DEGLACIAL ICE FLOW SWITCHING & ICE MARGIN ISOLATION

c LOCALISED ICE STAGNATION AND DOWNWASTING

d LATE STAGE ACTIVE MARGIN RETREAT

940 **Figure 7: Schematic model of the geomorphic imprint associated with the terrestrial ice sheet margin collapse of the southwestern Laurentide Ice Sheet. (a) Shows initial ice margin retreat in the outer deglacial zone where large recessional moraines are produced. Large ice streams feed the margin and are aligned with the direction of marginal retreat. (b) Shows deglacial ice flow switching and reorganization resulting in the isolation of large regions of the ice sheet in the intermediate deglacial zone. (c) Ice sheet thinning and rapid retreat triggered large-scale ice stream reorganization resulting in the isolation of large regions of the ice sheet and ice sheet stagnation in the intermediate deglacial zone. (d) Shows late-stage active margin retreat of the inner deglacial zone juxtaposition with**
945 **punctuated ice sheet stagnation.**

950 **Table 1: Diagnostic criteria for identifying flowset types** (after Greenwood and Clark, 2009; Kleman et al., 1997; Stokes and Clark, 1999).

Flowset types	Characteristics
Ice stream	Represent corridors within an ice sheet that are flowing faster relative to the surrounding ice. Composed of groups of highly elongate glacial bedforms (i.e. flutes, drumlins and mega-scale glacial lineations) with abrupt lateral margins (in places marked by lateral shear moraines).
Event	Represent areas of the ice sheet that surround ice streams. They can form hundreds of kilometres inside the ice margin. Composed of groups of elongate glacial bedforms (i.e. flutes and drumlins). These flowsets are not associated with meltwater features, but may contain superimposed meltwater features, such as misaligned eskers. Misaligned meltwater features result from a subsequent phase of deglaciation and retreat, which are associated with different flowset geometries.
Deglacial retreat	Represent areas of the ice sheet composed of warm-based ice flow during phases of deglaciation. These flowsets are formed close to the ice margin and may be time-transgressive due to the inward migration of warm-based ice. Composed of elongate glacial bedforms, which are locally aligned with eskers and meltwater channels. These flowsets are often associated with terminal, recessional moraines or glaciotectonic thrust ridges.
Deglacial readvance	Represent areas where the localized retreat pattern has been cross-cut by another deglacial flowset. These flowsets represent areas of the ice sheet composed of warm-based ice during phases of deglaciation. In some cases these flowsets may represent switches between periods of rapid and slow ice flow driven by internal forcing mechanisms, in such cases we refer to them as exhibiting surge behaviour. Composed of groups of elongate glacial bedforms (i.e. flutes, drumlins), which are locally aligned with eskers and meltwater channels. These flowsets are often associated with terminal, recessional moraines or glaciotectonic thrust ridges.
Palimpsest	Represent areas that are overprinted by younger ice flows with older flow traces exhibiting a similar orientation. These flowsets are often fragments.
Unknown	The relative age and glaciodynamic implications of the flowsets are uncertain. These flowsets are often fragments or contain insufficient landforms to interpret their origin.